with Aβ *in vivo*. Tau phosphorylation and apoptosis were induced by Aβ in hippocampal cultures (42). Thus, as suggested by Stein *et al*, high intrahippocampal concentration of Aβ, induced temporarily by the disruption of TTR binding of Aβ by the antibody, might have caused localized neurodegeneration in the CA1 field. The neurodegeneration reportedly detected in the antibody-infused limited area of hippocampus of Tg2576 mice (42), however, was not detected in the entire brain of TTR-deficient Tg2576 mice.

Stein and Johnson reported that the lack of neurodegeneration was associated with increased level of TTR synthesized in the hippocampus of Tg2576 mice (43). However, Lazarov *et al* reported that the individual levels of TTR mRNA in the hippocampi of a transgenic mouse model of AD, which co-expresses familial AD-linked mutant APP, and presenilin 1 (PS1) cDNAs were considerably variable (20). Furthermore, it had been reported that choroid plexus is the sole site of TTR synthesis within the brain; in this regard, Sousa *et al* recently confirmed that TTR is not produced in the brain parenchyma of either wild-type or Tg2576 mice, using laser dissection microscopy (41). The finding suggests that contamination by choroid plexus might lead to misinterpretation of the role of TTR in Aβ deposition in the brain.

In the present study, we compared the onset and progression of Aβ pathology in TTR null Tg2576 (Tg2576/$TTR^{-/-}$) mice with those in heterozygous mutant Tg2576 mice (Tg2576$TTR^{+/-}$). Thus, one factor which causes the discrepancy between our data and other authors' data obtained by examining only Tg2576 mice homozygous for the wild-type *TTR* gene (Tg2576/$TTR^{+/+}$) for comparison might be the difference in the levels of TTR. However, the onset and progression of Aβ pathology in our Tg2576/$TTR^{+/-}$ mice are rather delayed than accelerated relative to those in Tg2576/$TTR^{+/+}$ mice previously reported by other authors (6, 18, 45, 55). Thus, the possibility that homozygous levels of TTR would be required to prevent Aβ pathology appears to be remote.

On the other hand, Nunes *et al* reported that peptidylglycine α-amidating monooxygenase, the rate-limiting enzyme in neuropeptide maturation, is over-expressed in the peripheral, and central nervous systems of $TTR^{-/-}$ mice that, consequently, display increased neuropeptide Y (NPY) levels relative to wild-type mice (28). NPY is known to be a substrate of neprilysin, which is an Aβ-degrading protease (50). Another Aβ-degrading enzyme, insulin-degrading enzyme (IDE) is also known as insulin and amylin protease (30, 50). Hyperinsulinaemia is known to increase the risk of developing AD. Thus, it is suggested that hyperinsulinaemia may elevate Aβ level through insulin's competition with Aβ for IDE (30). Analogous to the competition, the increase in NPY levels in $TTR^{-/-}$ mice might competitively reduce neprilysin clearance of Aβ. Thus, Tg2576/$TTR^{-/-}$ mice might display enhanced Aβ deposition relative to Tg2576/$TTR^{+/-}$ mice through NPY's competition with Aβ for neprilysin. Contrary to the expectation, Tg2576/$TTR^{-/-}$ mice display rather suppressed Aβ deposition relative to Tg2576/$TTR^{+/-}$ mice (Figures 2 and 4). The results say that TTR does not suppress but rather accelerates Aβ deposition in Tg2576 mice.

Contrary to our findings, Choi *et al* recently reported that in a different transgenic mouse model of AD heterozygous for the disrupted *TTR* gene ($TTR^{+/-}$), brain Aβ deposition is significantly accelerated relative to the age-matched model homozygous for the wild-type *TTR* gene ($TTR^{+/+}$) (8). Their observation, which suggests that TTR suppresses Aβ deposition, contradicts ours. It is important to note that there are several critical differences in the experimental designs which might have caused the contradiction between their data and ours: (i) the AD model mouse we examined (Tg2576) is distinct from that Choi *et al* examined. They used *ceAPPswe/PS1ΔE9* mice that harbor not only the human mutant APP cDNA with the double mutation K670N and M671L linked to a Swedish familial AD but also the human mutant PS1 cDNA with the exon 9 deletion linked to a familial AD (16, 21). In contrast to Tg2576 mice, their control singly transgenic mice that express the human mutant APP cDNA alone are free of brain Aβ deposits up to age 14 months and co-expression of human mutant APP, and PS1 accelerates the amyloid deposition (3, 21). Furthermore, comparative analysis of cortical gene expression patterns between Tg2576 mice homozygous for the PS1 knock-in mutation (Tg2576/$PS1^{P264L/264L}$) and control Tg2576 mice heterozygous for the PS1 mutation (Tg2576/$PS1P^{264L/+}$) by DNA micro-array analysis revealed that the patterns are distinct, although there were some common regulated genes (54). All these observations suggest that the molecular pathogenesis of Aβ deposition in the two mouse models is different; (ii) the level of human variant APP in the brain of Tg2576 mice is more than fourfold higher than that of endogenous brain APP (14). On the other hand, although the level of human variant APP in the brain of *ceAPPswe/PS1ΔE9* mice is not described (8), variant PS1ΔE9 reportedly elevates Aβ42/Aβ40 ratio (3). Thus the contradiction between their results and ours might be caused by the significant difference in the levels of Aβ42 and/or Aβ40 between Tg2576 and *ceAPPswe/PS1ΔE9* mice; and (iii) Choi *et al* compared the degree of Aβ deposition between the brains of *ceAPPswe/PS1ΔE9* mice heterozygous for the disrupted *TTR* gene ($TTR^{+/-}$) and the mice homozygous for the wild-type *TTR* gene ($TTR^{+/+}$) (8), in contrast to the TTR null ($TTR^{-/-}$) and $TTR^{+/-}$ Tg2576 mice we examined for comparison. Thus in their study, in contrast to our study, the individual differences in the levels of brain TTR among the $TTR^{+/-}$ and control $TTR^{+/+}$ mice should critically affect the results, and hence, the elucidation of the relationship between TTR and Aβ deposition. They described that the levels of immunoreactive TTR in the extracts from the brains of *ceAPPswe/PS1ΔE9/*$TTR^{+/-}$ mice are clearly lower relative to the age-matched *ceAPPswe/PS1ΔE9/*$TTR^{+/+}$ mice at all ages examined (8). However, the report is lacking in important details about the levels of TTR in the individual animals that would make the data more compelling. For example, given only the pictorial data with sample number of 1, it is not clear that the differences in the brain levels of TTR between *ceAPPswe/PS1ΔE9/*$TTR^{+/+}$ and *ceAPPswe/PS1ΔE9/*$TTR^{+/-}$ mice are really significant. On the other hand, it is possible that TTR, as a peripheral Aβ binding protein, may have the ability to act as a peripheral Aβ 'sink'; whereby, it pulls Aβ from the brain into the periphery, hence decreasing the amount of Aβ in the brain (26, 33, 52, 56). Thus, if we had examined Tg2576$TTR^{+/+}$ mice, we, too, might have detected a decrease in Aβ deposition as Choi *et al* did.

All the above differences may cause the contradiction between their data and ours. Moreover, they described that the levels of brain TTR were significantly lower in human AD patients compared with age-matched controls and negatively correlated with the abundance of amyloid plaques. However, the references they cited didn't refer to the brain TTR levels but to the CSF TTR levels in the patients (8) and, to our knowledge, the comparison of the brain TTR levels between AD patients and control disease-free individuals has not yet been reported.

In conclusion, our results indicated, for the first time, TTR does not suppress but accelerates vascular Aβ burden in the brain of Tg2576 mice. However, the mechanism(s) by which TTR affects the Aβ deposition *in vivo* are not yet elucidated. Taken together with the Choi et al's contradictory finding (8), our finding suggests that the role of TTR in the pathogenesis of AD remains to be understood.

## ACKNOWLEDGMENTS

The authors would like to thank Drs. K. H. Ashe and Takaomi C. Saido for provision of Tg2576 mice and Ab9204 antibody, respectively. This work was supported by grants from the Ministry of Education, Culture, Sports, Science and Technology, Japan: Grants-in-aids for Scientific Research (18390098; to SM); and by grants to the Amyloidosis Research Committee for the Research on Intractable Diseases from the Ministry of Health, Labour and Welfare, Japan (to MS & SM).

## REFERENCES

1. Alonzo NC, Hyman BT, Rebeck GW, Greenberg SM (1998) Progression of cerebral amyloid angiopathy: accumulation of amyloid-beta40 in affected vessels. *J Neuropathol Exp Neurol* **57**:353–359.
2. Biroccio A, Del Boccio P, Panella M, Bernardini S, Di Ilio C, Gambi D *et al* (2006) Differential post-translational modifications of transthyretin in Alzheimer's disease: a study of the cerebral spinal fluid. *Proteomics* **6**:2305–2313.
3. Borchelt DR, Ratovitski T, van Lare J, Lee MK, Gonzales V, Jenkins NA *et al* (1997) Accelerated amyloid deposition in the brains of transgenic mice coexpressing mutant presenilin 1 and amyloid precursor proteins. *Neuron* **19**:939–945.
4. Botto M, Hawkins PN, Bickerstaff MC, Herbert J, Bygrave AE, McBride A *et al* (1997) Amyloid deposition is delayed in mice with targeted deletion of the serum amyloid P component gene. *Nat Med* **3**:855–859.
5. Braak H, Braak E (1991) Neuropathological stageing of Alzheimer-related changes. *Acta Neuropathol (Berl)* **82**: 239–259.
6. Carro E, Trejo JL, Gomez-Isla T, LeRoith D, Torres-Aleman I (2002) Serum insulin-like growth factor I regulates brain amyloid-beta levels. *Nat Med* **8**:1390–1397.
7. Castano EM, Prelli F, Soto C, Beavis R, Matsubara E, Shoji M, Frangione B (1996) The length of amyloid-beta in hereditary cerebral hemorrhage with amyloidosis, Dutch type. Implications for the role of amyloid-beta 1-42 in Alzheimer's disease. *J Biol Chem* **271**:32185–32191.
8. Choi SH, Leight SN, Lee VM, Li T, Wong PC, Johnson JA, Saraiva MJ, Sisodia SS (2007) Accelerated Abeta deposition in APPswe/PS1deltaE9 mice with hemizygous deletions of TTR (transthyretin). *J Neurosci* **27**:7006–7010.
9. Episkopou V, Maeda S, Nishiguchi S, Shimada K, Gaitanaris GA, Gottesman ME, Robertson EJ (1993) Disruption of the transthyretin gene results in mice with depressed levels of plasma retinol and thyroid hormone. *Proc Natl Acad Sci USA* **90**:2375–2379.
10. Giunta S, Valli MB, Galeazzi R, Fattoretti P, Corder EH, Galeazzi L (2005) Transthyretin inhibition of amyloid beta aggregation and toxicity. *Clin Biochem* **38**:1112–1119.
11. Hardy J, Selkoe DJ (2002) The amyloid hypothesis of Alzheimer's disease: progress and problems on the road to therapeutics. *Science* **297**:353–356.
12. Holtzman DM, Bales KR, Tenkova T, Fagan AM, Parsadanian M, Sartorius LJ *et al* (2000) Apolipoprotein E isoform-dependent amyloid deposition and neuritic degeneration in a mouse model of Alzheimer's disease. *Proc Natl Acad Sci USA* **97**:2892–2897.
13. Hsiao K, Chapman P, Nilsen S, Eckman C, Harigaya Y, Younkin S *et al* (1996) Correlative memory deficits, Abeta elevation, and amyloid plaques in transgenic mice. *Science* **274**:99–102.
14. Hsiao KK, Borchelt DR, Olson K, Johannsdottir R, Kitt C, Yunis W *et al* (1995) Age-related CNS disorder and early death in transgenic FVB/N mice overexpressing Alzheimer amyloid precursor proteins. *Neuron* **15**:1203–1218.
15. Irizarry MC, McNamara M, Fedorchak K, Hsiao K, Hyman BT (1997) APPSw transgenic mice develop age-related A beta deposits and neuropil abnormalities, but no neuronal loss in CA1. *J Neuropathol Exp Neurol* **56**:965–973.
16. Jankowsky JL, Slunt HH, Ratovitski T, Jenkins NA, Copeland NG, Borchelt DR (2001) Co-expression of multiple transgenes in mouse CNS: a comparison of strategies. *Biomol Eng* **17**:157–165.
17. Joachim CL, Duffy LK, Morris JH, Selkoe DJ (1988) Protein chemical and immunocytochemical studies of meningovascular beta-amyloid protein in Alzheimer's disease and normal aging. *Brain Res* **474**:100–111.
18. Kawarabayashi T, Younkin LH, Saido TC, Shoji M, Ashe KH, Younkin SG (2001) Age-dependent changes in brain, CSF, and plasma amyloid (beta) protein in the Tg2576 transgenic mouse model of Alzheimer's disease. *J Neurosci* **21**:372–381.
19. Kisilevsky R, Lemieux LJ, Fraser PE, Kong X, Hultin PG, Szarek WA (1995) Arresting amyloidosis in vivo using small-molecule anionic sulphonates or sulphates: implications for Alzheimer's disease. *Nat Med* **1**:143–148.
20. Lazarov O, Lee M, Peterson DA, Sisodia SS (2002) Evidence that synaptically released beta-amyloid accumulates as extracellular deposits in the hippocampus of transgenic mice. *J Neurosci* **22**:9785–9793.
21. Lazarov O, Robinson J, Tang YP, Hairston IS, Korade-Mirnics Z, Lee VM *et al* (2005) Environmental enrichment reduces Abeta levels and amyloid deposition in transgenic mice. *Cell* **120**:701–713.
22. Link CD (1995) Expression of human beta-amyloid peptide in transgenic Caenorhabditis elegans. *Proc Natl Acad Sci USA* **92**:9368–9372.
23. Ma J, Yee A, Brewer HB, Das S, Potter H (1994) Amyloid-associated proteins $\alpha_1$-antichymotrypsin and apolipoprotein E promote assembly of Alzheimer β-protein into filaments. *Nature* **372**:92–94.
24. Matsubara E, Bryant-Thomas T, Pacheco Quinto J, Henry TL, Poeggeler B, Herbert D *et al* (2003) Melatonin increases survival and inhibits oxidative and amyloid pathology in a transgenic model of Alzheimer's disease. *J Neurochem* **85**:1101–1108.
25. Matsubara E, Ghiso J, Frangione B, Amari M, Tomidokoro Y, Ikeda Y *et al* (1999) Lipoprotein-free amyloidogenic peptides in plasma are elevated in patients with sporadic Alzheimer's disease and Down's syndrome. *Ann Neurol* **45**:537–541.
26. Matsuoka Y, Saito M, LaFrancois J, Saito M, Gaynor K, Olm V *et al* (2003) Novel therapeutic approach for the treatment of Alzheimer's disease by peripheral administration of agents with an affinity to beta-amyloid. *J Neurosci* **23**:29–33.
27. Noda-Saita K, Terai K, Iwai A, Tsukamoto M, Shitaka Y, Kawabata S *et al* (2004) Exclusive association and simultaneous appearance of congophilic plaques and AT8-positive dystrophic neurites in Tg2576 mice suggest a mechanism of senile plaque formation and progression of neuritic dystrophy in Alzheimer's disease. *Acta Neuropathol (Berl)* **108**:435–442.
28. Nunes AF, Saraiva MJ, Sousa MM (2006) Transthyretin knockouts are a new mouse model for increased neuropeptide Y. *Faseb J* **20**:166–168.

29. Prelli F, Castano E, Glenner GG, Frangione B (1988) Differences between vascular and plaque core amyloid in Alzheimer's disease. *J Neurochem* **51**:648–651.
30. Qiu WQ, Folstein MF (2006) Insulin, insulin-degrading enzyme and amyloid-beta peptide in Alzheimer's disease: review and hypothesis. *Neurobiol Aging* **27**:190–198.
31. Rensink AA, de Waal RM, Kremer B, Verbeek MM (2003) Pathogenesis of cerebral amyloid angiopathy. *Brain Res Brain Res Rev* **43**:207–223.
32. Sadowski MJ, Pankiewicz J, Scholtzova H, Mehta PD, Prelli F, Quartermain D, Wisniewski T (2006) Blocking the apolipoprotein E/amyloid-beta interaction as a potential therapeutic approach for Alzheimer's disease. *Proc Natl Acad Sci USA* **103**:18787–18792.
33. Sagare A, Deane R, Bell RD, Johnson B, Hamm K, Pendu R *et al* (2007) Clearance of amyloid-β by circulating lipoprotein receptors. *Nat Med* **13**:1029–1031.
34. Saido TC, Iwatsubo T, Mann DM, Shimada H, Ihara Y, Kawashima S (1995) Dominant and differential deposition of distinct beta-amyloid peptide species, a beta N3(pE), in senile plaques. *Neuron* **14**:457–466.
35. Sasaki A, Shoji M, Harigaya Y, Kawarabayashi T, Ikeda M, Naito M *et al* (2002) Amyloid cored plaques in Tg2576 transgenic mice are characterized by giant plaques, slightly activated microglia, and the lack of paired helical filament-typed, dystrophic neurites. *Virchows Arch* **441**:358–367.
36. Schwarzman AL, Goldgaber D (1996) Interaction of transthyretin with amyloid beta-protein: binding and inhibition of amyloid formation. *Ciba Found Symp* **199**:146–160.discussion 60–64.
37. Schwarzman AL, Gregori L, Vitek MP, Lyubski S, Strittmatter WJ, Enghilde JJ *et al* (1994) Transthyretin sequesters amyloid beta protein and prevents amyloid formation. *Proc Natl Acad Sci USA* **91**:8368–8372.
38. Serot JM, Christmann D, Dubost T, Couturier M (1997) Cerebrospinal fluid transthyretin: aging and late onset Alzheimer's disease. *J Neurol Neurosurg Psychiatry* **63**:506–508.
39. Seubert P, Vigo-Pelfrey C, Esch F, Lee M, Dovey H, Davis D *et al* (1992) Isolation and quantification of soluble Alzheimer's beta-peptide from biological fluids. *Nature* **359**:325–327.
40. Shoji M, Golde TE, Ghiso J, Cheung TT, Estus S, Shaffer LM *et al* (1992) Production of the Alzheimer amyloid beta protein by normal proteolytic processing. *Science* **258**:126–129.
41. Sousa JC, Cardoso I, Marques F, Saraiva MJ, Palha JA (2007) Transthyretin and Alzheimer's disease: where in the brain? *Neurobiol Aging* **28**:713–718.
42. Stein TD, Anders NJ, DeCarli C, Chan SL, Mattson MP, Johnson JA (2004) Neutralization of transthyretin reverses the neuroprotective effects of secreted amyloid precursor protein (APP) in APPSW mice resulting in tau phosphorylation and loss of hippocampal neurons: support for the amyloid hypothesis. *J Neurosci* **24**:7707–7717.
43. Stein TD, Johnson JA (2002) Lack of neurodegeneration in transgenic mice overexpressing mutant amyloid precursor protein is associated with increased levels of transthyretin and the activation of cell survival pathways. *J Neurosci* **22**:7380–7388.
44. Suzuki N, Iwatsubo T, Odaka A, Ishibashi Y, Kitada C, Ihara Y (1994) High tissue content of soluble beta 1-40 is linked to cerebral amyloid angiopathy. *Am J Pathol* **145**:452–460.
45. Takeuchi A, Irizarry MC, Duff K, Saido TC, Hsiao Ashe K, Hasegawa M *et al* (2000) Age-related amyloid beta deposition in transgenic mice overexpressing both Alzheimer mutant presenilin 1 and amyloid beta precursor protein Swedish mutant is not associated with global neuronal loss. *Am J Pathol* **157**:331–339.
46. Tennent GA, Lovat LB, Pepys MB (1995) Serum amyloid P component prevents proteolysis of the amyloid fibrils of Alzheimer disease and systemic amyloidosis. *Proc Natl Acad Sci USA* **92**:4299–4303.
47. Togashi S, Lim SK, Kawano H, Ito S, Ishihara T, Okada Y *et al* (1997) Serum amyloid P component enhances induction of murine amyloidosis. *Lab Invest* **77**:525–531.
48. Tomidokoro Y, Harigaya Y, Matsubara E, Ikeda M, Kawarabayashi T, Shirao T *et al* (2001) Brain Abeta amyloidosis in APPsw mice induces accumulation of presenilin-1 and tau. *J Pathol* **194**:500–506.
49. Tomidokoro Y, Ishiguro K, Harigaya Y, Matsubara E, Ikeda M, Park JM *et al* (2001) Abeta amyloidosis induces the initial stage of tau accumulation in APP (SW) mice. *Neurosci Lett* **299**:169–172.
50. Wang DS, Dickson DW, Malter JS (2006) beta-Amyloid degradation and Alzheimer's disease. *J Biomed Biotechnol* **2006**:58406.
51. Wei L, Kawano H, Fu X, Cui D, Ito S, Yamamura K *et al* (2004) Deposition of transthyretin amyloid is not accelerated by the same amyloid in vivo. *Amyloid* **11**:113–120.
52. Weller RO, Cohen NR, Nicoll JA (2004) Cerebrovascular disease and the pathophysiology of Alzheimer's disease. Implications for therapy. *Panminerva Med* **46**:239–251.
53. Westerman MA, Cooper-Blacketer D, Mariash A, Kotilinek L, Kawarabayashi T, Younkin LH *et al* (2002) The relationship between Abeta and memory in the Tg2576 mouse model of Alzheimer's disease. *J Neurosci* **22**:1858–1867.
54. Wu ZL, Ciallella JR, Flood DG, O'Kane TM, Bozyczko-Coyne D, Savage MJ (2006) Comparative analysis of cortical gene expression in mouse models of Alzheimer's disease. *Neurobiol Aging* **27**:377–386.
55. Yang F, Lim GP, Begum AN, Ubeda OJ, Simmons MR, Ambegaokar SS *et al* (2005) Curcumin inhibits formation of amyloid beta oligomers and fibrils, binds plaques, and reduces amyloid in vivo. *J Biol Chem* **280**:5892–5901.
56. Zlokovic BV (2004) Clearing amyloid through the blood-brain barrier. *J Neurochem* **89**:807–811.

BRAIN RESEARCH 1214 (2008) 159–168

available at www.sciencedirect.com

ScienceDirect

www.elsevier.com/locate/brainres

BRAIN RESEARCH

Research Report

# Microglial activation in brain lesions with tau deposits: Comparison of human tauopathies and tau transgenic mice TgTau$^{P301L}$

*Atsushi Sasaki*[a,*], *Takeshi Kawarabayashi*[b], *Tetsuro Murakami*[c], *Etsuro Matsubara*[d], *Masaki Ikeda*[e], *Haruo Hagiwara*[f], *David Westaway*[g], *Peter S. George-Hyslop*[g], *Mikio Shoji*[b], *Yoichi Nakazato*[a]

[a] *Department of Human Pathology, Gunma University Graduate School of Medicine, Gunma, Japan*
[b] *Department of Neurology, Hirosaki University Graduate School of Medicine, Aomori, Japan*
[c] *Department of Neurology, Neuroscience, Biophysiological Science, Okayama University Graduate School of Medicine, Dentistry and Pharmaceutical Science, Okayama, Japan*
[d] *Department of Alzheimer's Disease Research, National Institute of Longevity Sciences, National Center for Geriatrics and Gerontology, Aichi, Japan*
[e] *Department of Neurology, Gunma University Graduate School of Medicine, Gunma, Japan*
[f] *Department of Anatomy and Cell Biology, Gunma University Graduate School of Medicine, Gunma, Japan*
[g] *Center for Research in Neurodegenerative Diseases, University of Toronto, Toronto, Ontario, Canada*

ARTICLE INFO

*Article history:*
Accepted 27 February 2008
Available online 8 March 2008

*Keywords:*
Microglia
Tau
Transgenic mice
Iba1
AT8
MHC class II

ABSTRACT

The aim of this study is to clarify the relationship of microglia to phosphorylated tau accumulation and the characteristics of microglial activation in brain lesions of human tauopathies in comparison to mutant tau transgenic (TG) mice. We performed immunocytochemical analyses of brains from six patients with tauopathies, and 24 mice (18 TG mice expressing mutant tau P301L and six non-TG control mice, 11 to 27 months of age) using anti-tau antibodies and various microglial markers. In the tau TG, both semiquantitative severity ratings of microglial activation and an ultrastructural study were performed. In human tauopathies, Iba1- and major histocompatibility complex (MHC) class II-positive activated microglia increased in regions of phosphorylated tau (AT8) accumulation. The immunoreactivity of scavenger receptor class A (SRA) was present in some activated microglia, including phagocytic microglia in Alzheimer's disease (AD). Double-immunofluorescent analysis under a confocal microscope showed activated microglia at the vicinity of AT8-positive cells. Semiquantitative data of the TG and control mice indicated that the immunopositivity of AT8 was closely associated with the number of Iba1-positive microglia in the cortical area. Tau-associated microglia showed rare immunoreactivity for MHC class II antigen and SRA in the TG mice. Ultrastructurally, activated microglia with enlarged cytoplasm were located near neurons containing abnormal cytoskeletons. This comparative study of human tauopathies and tau TG mice

* *Corresponding author.* Department of Human Pathology, Gunma University Graduate School of Medicine, 3-39-22 Showa-machi, Maebashi, Gunma 371-8511, Japan.
E-mail address: achie@med.gunma-u.ac.jp (A. Sasaki).

0006-8993/$ – see front matter 
doi:10.1016/j.brainres.2008.02.084

indicated that microglial activation was closely related to phosphorylated tau accumulation, and that activated microglia of the TG mice may have the low expression of MHC class II and SRA compared with those of human tauopathies.



## 1. Introduction

The abnormal hyperphosphorylation of tau is a feature common to all diseases with tau filaments. The tau-immunopositive deposits are present in the tau-associated disorders, tauopathies, such as progressive supranuclear palsy (PSP), Pick's disease (PiD), corticobasal degeneration (CBD), frontotemporal dementia and parkinsonism linked to chromosome 17 (FTDP-17). The tauopathies have been characterized by their biochemical features. It has been reported that three-repeat (3R)-tau isoforms predominantly aggregate into filaments in PiD while four-repeat (4R)-tau isoforms aggregate into filaments in PSP and CBD (Buee and Delacourte, 1999). The tau isoform composition of Alzheimer's disease (AD) is a variable mixture of 3R- and 4R-tau (Greenberg and Davies, 1990). The monoclonal antibodies RD3 and RD4 could distinguish the closely related 3R-tau and 4R-tau isoforms with complete specificity (de Silva et al., 2003). The antibody, ET3, is a 4R-tau-specific antibody (Fujino et al., 2005). In non-AD

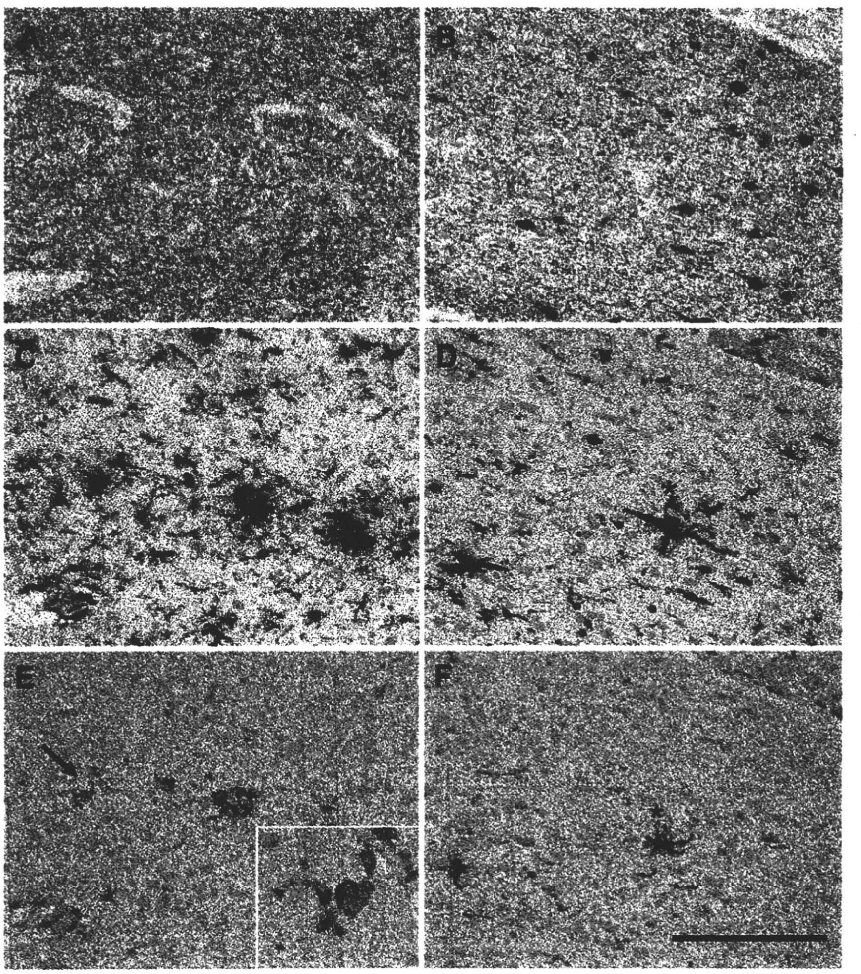


**Fig. 1 – Immunohistochemical study of AT8 (A, B), CR3.43 (C, D), and SRA (E, F) on adjacent sections of the frontal cortex of Alzheimer's disease (AD) (A, C, E) and the insular cortex of Pick's disease (PiD) (B, D, F,). The number of MHC class II-positive, activated microglia was much higher than that of SRA-positive microglia in both diseases. When we enlarged the area of AD cortex indicated by the arrow, a small number of SRA-positive, phagocytic microglia were found around senile plaques (E). The asterisks in panel D, F points to highly activated microglia labeled with MHC II and SRA in PiD. All sections were counterstained with hematoxylin. Scale bar=200 μm.**

human tauopathies, abnormal accumulation of tau protein has been shown not only in neurons, but also in glial cells such as astrocytes and oligodendrocytes. The formation of microglial inclusion bodies immunolabeled with phosphorylation-dependent monoclonal antibodies such as AT8 has not been reported in tauopathies, although the expression of tau2 and tau66 in microglia has been reported (Odawara et al., 1995; Ghoshal et al., 2001).

Microglial activation has been reported in a number of AD and transgenic (TG) mouse models of amyloid deposition, including Tg2576 (Frautschy et al., 1998). In AD brains, clusters of activated microglia with MHC class II expression can be found in fibrillary neuritic plaques and to a limited extent in diffuse plaques (Itagaki et al., 1989; Sasaki et al., 1997), and in APP Tg mice, activated microglia are observed around fibrillary Aβ deposits (Sasaki et al., 2002; Morgan et al., 2005). A previous study (Ishizawa and Dickson, 2001) demonstrated the expression of MHC class II molecules in activated microglia in the brains of PSP and CBD. The presence of MHC-positive, activated microglia in the non-AD tauopathies may support the argument that neuroinflammation contributes to pathogenesis of tauopathies. However, it is suggested that neuroinflammation in PSP and CBD is linked to tau pathology in a complicated way, and the pathogenic role of microglia and neuroinflammation may be different in multiple sclerosis, AD or non-AD tauopathies. Increasingly, it is necessary to examine multiple microglial markers from different activation state categories to obtain a more complete picture of the in vivo microglial phenotype. At present, information on microglial activation in non-Alzheimer's tauopathies as well as mutant tau transgenic (TG) mouse models is limited, particularly in the latter condition.

Microglia activation could occur in not only neurodegenerative diseases but also various diseases including local trauma, focal and global ischemia, local and generalized infection, immune-mediated inflammation, and brain tumors. The factors other than tau accumulation that induce

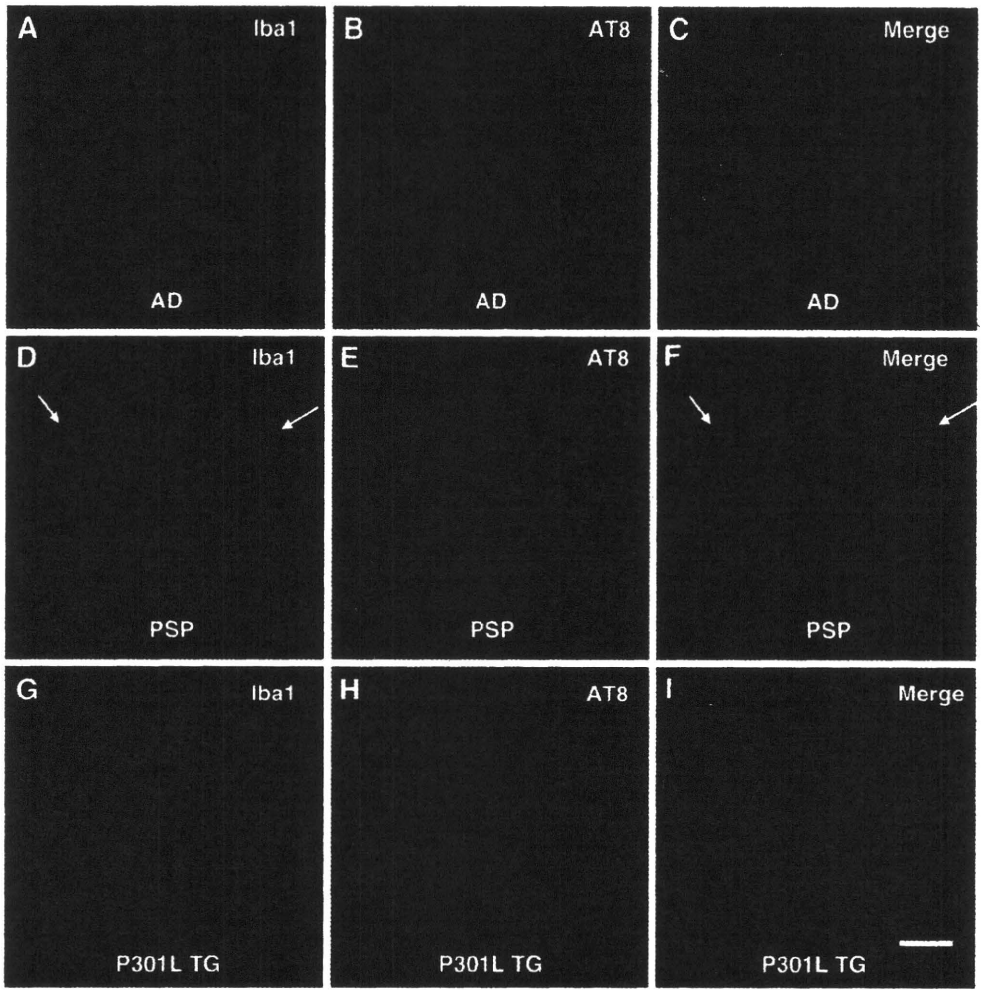


**Fig. 2 – Double immunofluorescence of Iba1 and AT8 under a confocal laser microscope in AD (A–C), PSP (D–F), and tau P301L TG mice (G–I). AT8 was absent in microglia, and microglial cluster surrounding AT8-positive cells (a focal accumulation of microglia around AT8-positive structures) was not evident. Arrows (D, F) points to activated microglia in PSP. Scale bar = 50 μm.**

microglial activation seem much fewer in the tau TG mice than in human autopsy cases of tauopathies. Therefore, the tau TG mice could be useful to clarify the relationship between phosphorylated tau accumulation and microglial alterations in brain lesions.

In the present study, we investigated human tauopathies and tau TG mice by immunohistochemistry and electron microscopy using anti-tau antibodies including 3R-/4R-specific antibodies and various microglial markers. The aim of this study to investigate: 1) the spatial correlation between microglial activation and tau accumulation; 2) the comparison of tau TG mice to human tauopathies with respect to the microglial shape and the production of microglial neuroinflammatory mediators.

## 2. Results

### 2.1. *Human tauopathies*

Iba1- and MHC class II-positive activated microglia increased in regions of phosphorylated tau accumulation in all the cases of human tauopathies. In the frontal cortex of AD (Figs. 1A,C,E) and the insular cortex of PiD (Figs. 1B,D,F), the number of MHC class II-positive, activated microglia was much larger than that of SRA-positive microglia in the adjacent sections stained with AT8, CR3.43, and SRA antibodies. Higher magnification showed a small number of SRA-positive, phagocytic microglia around senile plaques in AD (Fig. 1D, inset). The number of inducible nitric oxide synthase (iNOS)-positive microglial cells was very limited in each tauopathy case (data not shown).

In the frontal cortex of AD (Figs. 2A–C) and the periaqueductal grey matter of PSP (Figs. 2D–F), double immunofluorescence analysis showed different localizations of the Iba1 and AT8, and double-positive cells were not evident. In addition, there was no evidence of microglial clusters around cells bearing AT8-positive structures such as NFTs, pretangles and neuropil threads, or a direct attachment of activated microglia to tau accumulation.

### 2.2. *P301L tauTG mice*

At 11 months of age, weak tau staining appeared in the neocortex in one of four TG mice. By 17 months of age, tau-positive neuronal and glial structures were almost consistently observed, and memory disturbance developed, although there was phenotypic variation among the tau TG mice between 11 and 27 months. The hippocampus of the TG mice was labeled with AT8, and 4-repeat tau antibodies, ET3 and RD4, but not with 3-repeat antibody, RD3 (data not shown). In the cerebral cortical section of a 17-month-old P301L TG mouse, microglia were increased in cortical areas where AT8-positive, ET3-positive neuronal structures accumulated, while there was no apparent increase of microglial cells labeled with Iba1 antibody or RCA1 lectin in the areas of mild tau deposition (data not shown). There were no significant differences about the relationship between tau deposition and microglial activation with respect to anatomical regions. The increased microglia labeled with the microglial markers (Iba1 and RCA1) showed morphologically mild activation, revealed by the cytoplasmic enlargement, in the TG mice. The data of semiquantitative evaluation of tau and microglial pathology in cerebral cortical areas of 18 P301L TG mice and six controls are shown in Table 2. There was a positive correlation between the expression score of AT8 and Iba1, $r=0.781$ ($p<0.01$).

Double-immunofluorescent confocal laser microscopy showed an increased number of microglia in the cerebral cortex of TG mice with severe tau deposition, and the absence of tau immunoreactivity in microglia (Figs. 2G–I). Concerning the microglial shape and density, microglia with bushy processes increased in the areas, where AT8-positive cells were sparse, and microglial cluster was not evident around AT8-positive cells.

In the cryostat sections of the hippocampal area of 21-month-old tau TG mice, AT8-positive neurons/glia increased, and mildly activated microglia showed immunopositivity for Mac1 and F4/80, but only rarely for scavenger receptor class A (SRA) (Figs. 3A–D). A small number of Ia-positive microglia were observed in the area with severe AT8 deposition (Figs. 3E, F). We

Table 1 – Antibodies and lectin used in this study

| Specificity, epitope | Clone name, type | Source | Dilution | AR |
|---|---|---|---|---|
| Tau, phosphorylated S202/T205 | AT8, mouse MA | Innogenetics, Ghent, Belgium | 1/1000–1/200 | – |
| Tau, 3-repeat RD3 | 8E6/C11, mouse MA | Upstate, Lake Placid, NY, USA | 1/3000 | + |
| Tau, 4-repeat RD4 | 1E1/A6, mouse MA | Upstate, Lake Placid, NY, USA | 1/200 | + |
| Tau, 4-repeat | ET3, mouse MA | Dr. P. Davies | 1/1000 | + |
| Iba1 | Rabbit PA | Wako, Osaka, Japan | 1/500 | + |
| Human MHC class II, beta-chains of DP, DQ and DR | CR3.43, mouse MA | DAKO, Glostrup, Denmark | 1/50 | + |
| Mouse MHC class II (Ia), I-A and I-E | M5/114, rat MA | Behringer-Mannheim, Mannheim, Germany | 1/20 | – |
| Human SRA, CD204 | SRA-E5 | Trans Gene Inc., Kumamoto, Japan | 1/50 | + |
| Mouse SRA | 2F8, rat MA | Dr. S. Gordon | 1/250 | – |
| Human iNOS | Rabbit PA | CHEMICON, Temecula, CA, USA | 1/2000 | + |
| Rat and mouse iNOS | Rabbit PA | CHEMICON, Temecula, CA, USA | 1/5000 | – |
| CR3, CD11b and CD18 | Mac-1, rat MA | Behringer-Mannheim, Mannheim, Germany | 1/20 | – |
| Biotinylated RCA1 | β-d-Galactose | Vector, Burlingame, CA, USA | 1/200 | + |

Iba1, ionized calcium binding adaptor molecule 1; MHC, major histocompatibility complex; SRA, scavenger receptor class A; iNOS: inducible nitric oxide synthase; CR, complement receptor; RCA1, *Ricinus communis agglutinin* 1; AR: antigen retrieval; (+): autoclaving (121 °C, 10 min, citrate buffer).

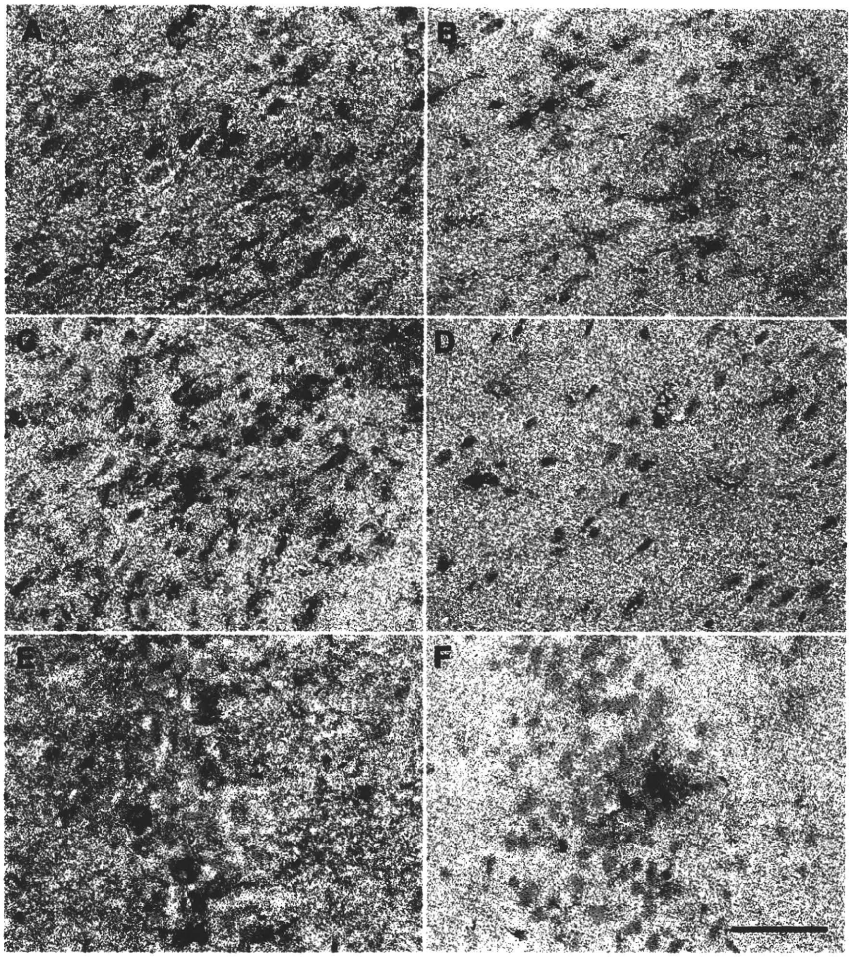


**Fig. 3 – Immunohistochemistry in the hippocampus of 21-month-old tau TG mice. Microglia with mild enlargement of their cytoplasm, labeled with Mac1 (B) and F4/80 (C) but rarely labeled with SRA (D), were observed in the subiculum with severe AT8 deposition (A). The pyramidal cell layer with numerous AT8-positive cells (E) had a small number of Ia-positive microglia (F). All the sections were counterstained with hematoxylin. Scale bar = 50 μm.**

could not find iNOS reactivity in the transgenic mice (data not shown).

In the ultrastructural analysis of the tau TG mice, we could see microglial cells, which had a small nucleus with dense peripheral chromatin and significantly enlarged cytoplasm containing increased rough endoplasmic reticulum and mitochondria, near neuron containing NFT-like structures (Fig. 4A). Immunoelectron microscopy using Iba1 antibody in P301L TG mice revealed that the cytoplasm of Iba1-immunopositive microglia was filled with lysosomal dense bodies (Fig. 4B). Abnormal filamentous or tubular structures corresponding to NFTs were not found in microglia.

## 3. Discussion

The present study showed that P301L tau TG mice displayed microglial activation in the grey matter associated with phosphorylated tau deposition similar to those observed in human tauopathies. These include the increase of Iba1-positive microglia and the appearance of microglia expressing MHC class II antigen. Our semiquantitative analysis in the TG mice also demonstrated that the number of Iba1-positive microglia was closely associated with the accumulation of phosphorylated tau. Thus, our findings indicate that microglial activation may be involved in the progression of tauopathies.

This study illustrated the presence of activated microglia expressing Iba1, Mac1, F4/80, RCA-1 lectin and MHC class II protein (Ia antigen) in brain lesions rich in tau phosphorylation in P301L TG mice, which were generated by us as tau mutant (P301L) transgenic mice expressing an FTDP-17 mutation within the longest form of tau (2N, 4R) (Murakami et al., 2006). This is the first study to demonstrate multiple microglial markers in tau TG mice. By 17 months of age, tau-positive neuronal and glial structures were almost consistently observed, and memory disturbance developed. However, there is a general feature of phenotypic variation among our transgenic animal lines, as observed in this study. In other P301L TG mice, progressive white matter pathology (Lin et al.,

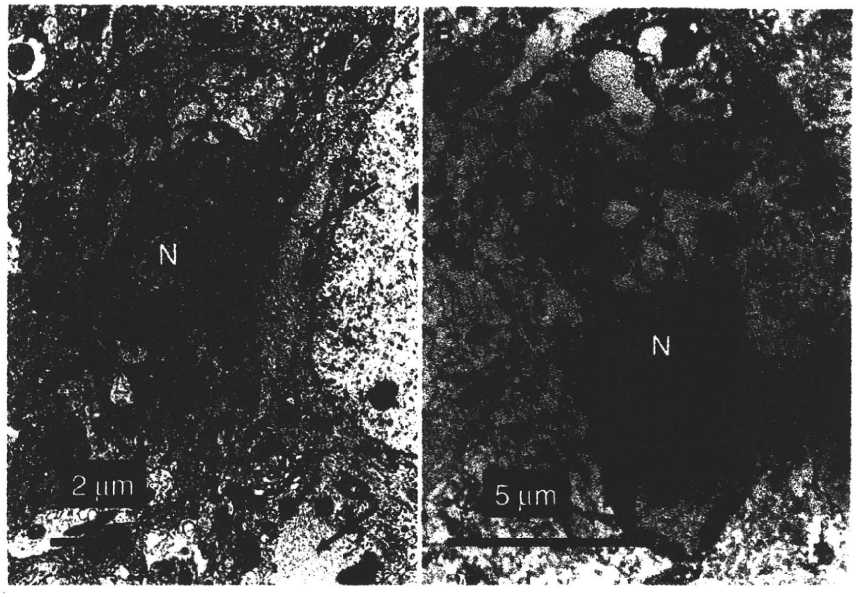


**Fig. 4–Ultrastructurally, microglial cells showed activation with slightly enlarged cytoplasm and lysosomal, dense bodies in the hippocampus of P301L mice (21-month-old). (A) Microglia with significantly enlarged cytoplasm containing increased rough endoplasmic reticulum and mitochondria were found near neurons containing abnormal, tubular structures (arrows). (B) Iba1 immunostaining revealed labeling of microglial cells filled with lysosomal dense bodies. No abnormal filamentous or tubular structures were observed in microglia. N: Nuclei of microglia.**

2005), gene expression profiles (Ho et al., 2001) and apoptosis (Zhao et al., 2003) have been examined. Microgliosis has been reported in some lines of TG mice expressing mutant tau, such as P301S (Bellucci et al., 2004) and R406W (Ikeda et al., 2005); however, the microglial pathology in TgTau$^{P301L}$ mice had not been investigated in detail in previous studies.

Our results of human tauopathies confirmed the findings of the previous reports that MHC class II-positive, activated microglia were present in some areas with tau burden in AD and non-AD tauopathies (Paulus et al., 1993; Kobayashi et al., 1999; Arnold et al., 2000; Ishizawa and Dickson, 2001). Regarding MHC class II protein expression, the expression in our tau TG mice seemed less marked than that in non-AD tauopathies. This might be related to the difference of the species and TG mouse model, since MHC class II expression is much less easily induced on microglia in the mouse (Perry, 1998) and microglia in TG mice overexpressing beta amyloid protein are less highly activated than those in human AD (Schwab et al., 2004). Another possibility is that microglial MHC class II expression is in part attributable to factors such as hypoxia or infection prior to patient death.

The present study demonstrated the different expression of SRA on microglia in AD, non-AD tauopathies, and P301L TG mice. A small cluster of phagocytic microglia expressing SRA could be observed around the senile plaques in AD, while cluster formation of phagocytic microglia was not evident in PiD or PSP. Bornemann et al. (2001) demonstrated increased immunoreactivity for SRA on the borders of beta amyloid deposits in the TG mice overexpressing the amyloid precursor protein. Thus, increased expression of SRA on microglia might be due to extracellular deposits of beta amyloid in AD. So far, SRA expression of microglia in non-AD tauopathies and tau TG mice is unclear. The expression of SRA is not found in resting microglia, but in activated microglia, preferentially in phagocytic microglia. This phenomenon may be attributable to our observation that SRA was expressed in highly activated microglia in PiD. Alternatively, the expression of SRA on microglia was very rare in P301L TG mice in this study. There may be a difference between non-AD tauopathies and tau TG mice with respect to microglial SRA expression. In addition, morphological study made in this study indicated that the presence of phagocytic microglia (brain macrophages) was not evident in P301L TG mice. However, those findings do not rule out phagocytic activity of microglia in the TG mice model, since SRA is not the only marker for a microglial phagocytic phenotype (e.g., expression of Fc receptors is also generally considered to suggest phagocytic capability) and our electron microscopic evaluation of P301L TG mice identified numerous secondary lysosomes in microglia.

In the present study, there was no evidence of microglial clusters or attachment around neurons containing pretangles, NFTs, Pick bodies or neuropil threads in both tauopathies and the TG mice by immunoperoxidase and double immunofluorescence analyses using antibodies, such as AT8, Iba1, MHC class II, and SRA. The trigger for microglial activation in tauopathies still remains unclear. *In vitro* studies have investigated the effect of microglial stimulators, including lipopolysaccharide, interferon-gamma (IFN-gamma) and colony stimulating factors, and IFN-gamma has been shown to be a particularly potent microglial stimulant (Sasaki et al., 1989). However, no evidence of IFN-gamma stimulation on microglial activation has been reported in vivo, except in a study of multiple sclerosis

(Takeuchi et al., 2006). *In vitro* studies have shown that microglia are activated by beta amyloid (Lue et al., 2001), prion protein (Brown et al., 1996), and alpha-synuclein (Zhang et al., 2005); however, the effect of tau in microglial activation in culture systems is not yet known. In vivo the deposition of phosphorylated tau is intracellular except ghost tangles. Thus, the activation of microglia in tauopathies might result from a mediator such as ATP or cytokines/chemokines produced locally, not from direct interaction with phosphorylated tau.

The present study indicated that phosphorylated tau epitope (AT8) was absent in microglia, as shown by double-immunofluorescent confocal microscopy using Iba1 antibody, which is the most sensitive marker for microglia. Microglia labeled with monoclonal antibodies against conformational epitope of tau, tau2 and tau66, has been noted in AD, PSP, CBD, and in Lewy body disease (Odawara et al., 1995; Ghoshal et al., 2001). The expression of tau2 and tau66 in microglia does not seem to be disease-specific, since tau2-reactive microglia has been observed around ischemic foci of cerebral infarction and in inflammatory lesions of different pathologies (Uchihara et al., 2000, 2005). In addition, microglial cells are not labeled with Tau1, Alz50, or AD2, all of which reveal astrocytic and oligodendroglial pathology. No AT8-positive microglia were observed in PiD in sections subsequently stained with HLA-DR antibody (Schofield et al., 2003). The lack of AT8 in microglia might be due to the difference of cell origin and/or a paucity of molecules associated with microtubules. However, it is conceivable that the absence of phosphorylated tau or NFTs in microglia may not be indicative of functional normal microglia, since microglia become dysfunctional with aging and the deterioration of microglia is aggravated by genetic and environmental risk factors.

Importantly, what role activated microglia play in the pathogenesis and disease process of tauopathies should be addressed. The bystander damage hypothesis claiming microglial autotoxicity leaves unanswered issues in chronic CNS neurodegenerative diseases. However, microglia may play an important role in amplification of neuronal injury in tauopathies, and microglial dysfunction, "diseased microglial cells", may contribute to the slow degeneration of neurons and astrocytes. It is of particular significance that in the CNS, iNOS expression has been shown to provoke neuronal cell death. This study indicated that the expression of iNOS in activated microglia is not significant in tauopathies and P301L TG mice, in agreement with the results of PSP (Komori et al., 1998). Our immunocytochemical and electron microscopical results that activated microglia were present at the vicinity of tau-positive neurons suggest that activated microglia might be involved in microglial–neuronal interactions at the proximal neurites and synapses of the affected cells. An understanding of the role of microglia in synaptic signaling is still elusive, but microglia may play an important role like synaptic stripping (Trapp et al., 2007), N-methyl-D-aspartate (NMDA) receptor-mediated synaptic responses (Moriguchi et al., 2003) and releasing extracellular signaling molecules. Microglia may produce not only a direct toxic or trophic effect to neuron, but also an indirect one through the effect of astrocytic potential function in synapse. Recently, Yoshiyama et al. (2007) have shown that synapse loss, impaired synaptic function and microglial activation precede tangle formation in P301S TG mice, where tau pathology accelerated compared to P301L TG. In fact, it is the loss of synaptic contact that leads directly to the personal devastation, i.e. dementia (Terry, 2000). Thus, microglial activation might be early manifestation of neurodegeneration or neuroinflammation, and might be involved in dysfunction of synaptic signaling in tauopathies. Our P301L TG mice were reported to demonstrate memory disturbance at 11–12 months of age (Murakami et al., 2006). This study using immunohistochemistry and Iba1 antibody could not demonstrate that microglial response precedes the appearance of AT8 immunoreactivity or memory disturbance. To address the question of when microglial activation occurs, a further study of microglial pathology using morphologic and morphometric techniques in many P301L TG mice of young age groups should be performed.

In neurodegenerative diseases, different "activation states" of microglia exist in which microglia may selectively upregulate neuroprotective and/or neurotoxic molecules and depend on the activation environment, including the cell type and signal molecules. Yoshiyama et al. (2007) reported that activated microglia may be neurotoxic because immunosuppression with FK506 attenuated tau pathology and increased lifespan. Microglial production of trophic molecules, such as glia-derived neurotrophic factor and brain-derived neurotrophic factor, and neurotoxic molecules, such as NO and proinflammatory cytokines, as well as neuronal survival should be investigated quantitatively in tau TG mice, including FK-506-treated tau TG mice. Combined with our previous study (Murakami et al., 2006), this study suggests that microglial production of "trophic effectors" may be not enough to rescue injured neurons at the advanced stage of tauopathies.

In conclusion, microglial activation may be closely related to phosphorylated tau accumulation and a direct contribution of intracellular tau accumulation to the activation of neighboring microglia seems unlikely in human tauopathies and tau TG mice. The presence of activated microglia in the vicinity of tau-bearing neurons suggests that microglia might be involved in microglia–neuronal interaction at the proximal neurites or synapse. The present study serves to validate P301L TG mouse models of tauopathies with respect to microglial pathology. Based on the immunohistochemistry for Iba1, MHC class II and SRA, however, it appears that microglia of the TG mice have weak inflammatory response and low phagocytic activity compared with those of human tauopathies.

## 4. Experimental procedures

### 4.1. *Human tauopathies*

Autopsy brains from three AD patients (66, 71, 83 years old at death; two males and one female), two PSP patients (63 and 77 years old, two males) and one PiD patient (a 73-year-old male) were examined according to the ethical rules of Gunma University and the Japanese Society of Pathology. All brains were fixed in 10% buffered formalin, and embedded in

paraffin. For light microscopy and immunohistochemistry, consecutive 5-μm-thick sections, each containing one of the following regions, were studied: cerebral cortex and its subcortical white matter; hippocampus; basal ganglia and insular cortex; mid brain.

### 4.2. *TG mice expressing P301L human tau*

The TG mice for human mutant tau, P301L tau (proline to leucine mutation at the amino acid number 301 in exon 10), used in this study have been described previously (Murakami et al., 2006). We studied a total of 24 P301L TG mice (eight males and 16 females) between 11 months and 27 months of age. Six non-transgenic littermates (11–27 months old; two male and four females) served as controls. The animals were sacrificed and the brains were immediately excised and processed according to the following procedure. For histological and immunohistochemical analyses, all mouse brains were fixed in 0.1 M phosphate buffer (PB, pH 7.6) containing 4% paraformaldehyde (PFA), and embedded in paraffin. Then, consecutive sections were cut at 5-μm-thick. Some mouse brains were fixed with periodate–lysine–PFA (PLP) fixative at 4 °C for 4–6 h, washed with PBS and embedded in OCT compound (Miles, Elkhart, USA). The samples were cut into 6–8-μm-thick sections using a cryostat (Leica).

### 4.3. *Immunocytochemical methods*

Immunohistochemistry was performed using the biotin–streptavidin (B–SA) immunoperoxidase method (Nichirei, Tokyo, Japan). For staining of paraffin sections with some antibodies, antigen retrieval was performed by autoclaving (121 °C, 10 min, citrate buffer). The sections were incubated with each of the primary antibodies or biotinylated RCA-1 listed in Table 1 overnight at 4 °C. All sections, except those stained with RCA-1, were incubated with a secondary antibody at room temperature (RT) for 30 min, and then reacted with peroxidase-labeled streptavidin at RT for 30 min. The immunoreaction was visualized with diaminobenzidine (DAB) and briefly counterstained with hematoxylin.

Immunohistochemical analyses for rat monoclonal antibodies against Mac-1, F4/80, Ia antigen, and SRA were performed only on cryostat-cut tissue sections. After incubation with the rat monoclonal antibodies, biotinylated goat anti-rat Ig (diluted 1:20, Tago, Inc., Camerillo, Calif) was used as a secondary antibody, followed by streptavidin–peroxidase complex (Nichirei).

For double immunofluorescence analyses, sections were incubated overnight at 4 °C in a cocktail of the Iba1 polyclonal antibody and the mouse AT8 antibody. After the incubation, a combination of secondary antibodies, Alexa 488-tagged goat anti-rabbit IgG (1:200; Molecular Probe, USA) and Alexa 594-tagged goat anti-mouse IgG (1:200; Molecular Probe) were applied for 30 min at room temperature. Prior to immunolabeling, auto-fluorescence of the lipofuscin granules was blocked with Sudan black B treatment. The sections were examined with a BioRad MRC-1024 confocal microscopic system. As a control, parallel sections treated under identical conditions except for omission of each primary antibody were used.

Table 2 – Semiquantitative evaluation of AT8 and Iba1 immunoreactivity in cerebral cortical areas of P301L TG and non-TG mice

| No | Mice | Age (months) | Sex | AT8 | Iba1 |
|---|---|---|---|---|---|
| 1 | Non-TG | 11 | M | 0 | 1 |
| 2 | Non-TG | 23 | M | 0 | 1 |
| 3 | Non-TG | 24 | F | 0 | 1 |
| 4 | Non-TG | 25 | F | 0 | 1 |
| 5 | Non-TG | 25 | F | 0 | 1 |
| 6 | Non-TG | 27 | F | 0 | 1 |
| 7 | P301L TG | 11 | F | 0 | 1 |
| 8 | P301L TG | 11 | F | 0 | 1 |
| 9 | P301L TG | 11 | M | 0 | 1 |
| 10 | P301L TG | 11 | M | 1 | 1 |
| 11 | P301L TG | 18 | F | 1 | 1 |
| 12 | P301L TG | 18 | M | 1 | 1 |
| 13 | P301L TG | 19 | F | 1 | 1 |
| 14 | P301L TG | 24 | M | 1 | 1 |
| 15 | P301L TG | 24 | M | 1 | 1 |
| 16 | P301L TG | 26 | F | 1 | 1 |
| 17 | P301L TG | 27 | F | 1 | 1 |
| 18 | P301L TG | 21 | F | 2 | 1 |
| 19 | P301L TG | 19 | F | 2 | 2 |
| 20 | P301L TG | 18 | F | 3 | 2 |
| 21 | P301L TG | 17 | M | 3 | 3 |
| 22 | P301L TG | 18 | F | 3 | 3 |
| 23 | P301L TG | 21 | F | 3 | 3 |
| 24 | P301L TG | 25 | F | 3 | 3 |

AT8: 0, absent; 1, mild; 2, moderate; 3, severe.
Iba1: 1, <10 positive nuclei; 2, 10–20 positive nuclei; 3, >20 positive nuclei at ×400 magnification.

### 4.4. *Ultrastructural analysis*

For the transmission electron microscopy (EM) and the pre-embedding method of immunoelectron microscopy, cerebral cortical tissues of a 21-month-old P301L mouse were processed as described previously (Sasaki et al., 2002). In the transmission EM analysis, ultrathin sections were cut, and then stained with uranyl acetate and lead acetate prior to EM observation. After immunostaining of the immunoelectron microscopy, the ultrathin sections were cut, and were examined using EM with/without staining with uranyl acetate.

### 4.5. *Semiquantitative analysis of immunolabeling*

Cerebral cortical areas of 14 P301L TG and five control mice were selected for semiquantitative evaluation of tau and microglial pathology. The score of AT8 deposits was assigned as follows: 0 = absent, 1 = mild, 2 = moderate and 3 = severe. For microglial pathology, the microscopic field with the highest density of Iba1-positive microglia was identified and the number of microglia was counted at ×400 magnification. The score was determined as follows: 1=<10 cells, 2=10–20 cells, 3=>20 cells. In this assessment, each microglia had to have an immunopositive nucleus to be counted. Spearman correlation coefficients using a software (SPSS11.5 soft package for Windows) were used to evaluate whether the AT8 immunoreactivity was correlated with the Iba1 immunoreactivity.

## Acknowledgments

We thank Dr. Manuel Graeber for reviewing the manuscript. The expert technical assistance of Machiko Yokota and Kohji Isoda is gratefully acknowledged. This work was supported by Grants-in-Aid for Scientific Research (C) (18500276) from the Ministry of Education, Culture, Sports, Science and Technology, Japan, by Grants-in-Aid for the Primary Amyloidosis Research Committee (Yamada M) from the Ministry of Health, Labor and Welfare of Japan, by Grants-in-Aid for Scientific Research (B) (16390251), the National Project on Protein Structural and Functional Analyses and Scientific Research on Priority Areas (C)–Advanced Brain Science Project–from the Ministry of Education, Culture, Sports, Science and Technology, Japan.

## REFERENCES

Arnold, S.E., Han, L.-Y., Clark, C.M., Grossman, M., Trojanowski, J. Q., 2000. Quantitative neurohistological features of frontotemporal degeneration. Neurobiol. Aging 21, 913–919.

Bellucci, A., Westwood, A.J., Ingram, E., Casamenti, F., Goedert, M., Spillantini, M.G., 2004. Induction of inflammatory mediators and microglial activation in mice transgenic for mutant human P301S tau protein. Am. J. Pathol. 165, 1643–1652.

Bornemann, K.D., Wiederhold, K.H., Pauli, C., Ermini, F., Stalder, M., Schnell, L., Sommer, B., Jucker, M., Staufenbiel, M., 2001. Abeta-induced inflammatory processes in microglia cells of APP23 transgenic mice. Am. J. Pathol. 158, 63–67.

Brown, D.R., Schmidt, B., Kretzschmar, H.A., 1996. Role of microglia and host prion protein in neurotoxicity of a protein fragment. Nature 380, 345–347.

Buee, L., Delacourte, A., 1999. Comparative biochemistry of tau in progressive supranuclear palsy, corticobasal degeneration, FTDP-17 and Pick's disease. Brain Pathol. 9, 681–693.

de Silva, R., Lashley, T., Gibb, G., Hanger, D., Hope, A., Reid, A., Bandopadhyay, R., Utton, M., Strand, C., Jowett, T., Khan, N., Anderton, B., Wood, N., Holton, J., Revesz, T., Lees, A., 2003. Pathological inclusion bodies in tauopathies contain distinct complements of tau with three or four microtubule-binding repeat domains as demonstrated by new specific monoclonal antibodies. Neuropathol. Appl. Neurobiol. 29, 288–302.

Frautschy, S.A., Yang, F., Irrizarry, M., Hyman, B., Saido, T.C., Hsiao, K., 1998. Microglial response to amyloid plaques in APPsw transgenic mice. Am. J. Pathol. 152, 307–317.

Fujino, Y., Wang, D.-S., Thomas, N., Espinoza, M., Davies, P., Dickson, D.W., 2005. Increased frequency of argyrophilic grain disease in Alzheimer disease with 4R tau-specific immunohistochemistry. J. Neuropathol. Exp. Neurol. 64, 209–214.

Ghoshal, N., Garcia-Sierra, F., Fu, Y., Beckett, L.A., Mufson, E.J., Kuret, J., Berry, R.W., Binder, L.I., 2001. Tau-66: evidence for a novel tau confirmation in Alzheimer's disease. J. Neurochem. 77, 1372–1385.

Greenberg, S.G., Davies, P., 1990. A preparation of Alzheimer paired helical filaments that displays distinct tau proteins by polyacrylamide gel electrophoresis. Proc. Natl. Acad. Sci. U. S. A. 87, 5827–5831.

Ho, L., Xiang, Z., Mukherjee, P., Zhang, W., De Jesus, N., Mirjany, M., Yemul, S., Pasinetti, G.M., 2001. Gene expression profiling of the tau mutant (P301L) transgenic mouse brain. Neurosci. Lett. 310, 1–4.

Ikeda, M., Shoji, M., Kawarai, T., Kawarabayashi, T., Matsubara, E., Murakami, T., Sasaki, A., Tomidokoro, Y., Ikarashi, Y., Kuribara, H., Ishiguro, K., Hasegawa, M., Yen, S.-H., Chishti, M.A., Harigaya, Y., Abe, K., Okamoto, K., George-Hyslop, P., Westaway, D., 2005. Accumulation of filamentous tau in the cerebral cortex of human tau R406W transgenic mice. Am. J. Pathol. 166, 521–531.

Ishizawa, K., Dickson, D.W., 2001. Microglial activation parallels system degeneration in progressive supranuclear palsy and corticobasal degeneration. J. Neuropathol. Exp. Neurol. 60, 647–657.

Itagaki, S., McGeer, P.L., Akiyama, H., Zhu, S., Selkoe, D., 1989. Relationship of microglia and astrocytes to amyloid deposits of Alzheimer's disease. J. Neuroimmunol. 24, 173–182.

Kobayashi, K., Hayashi, M., Fukutani, Y., Miyazu, K., Shiozawa, M., Muramori, F., Aoki, T., Koshino, Y., 1999. KP1 expression of ghost Pick bodies, amyloid P-positive astrocytes and selective nigral degeneration in early onset Pick disease. Clin. Neuropathol. 18, 240–250.

Komori, T., Shibata, N., Kobayashi, M., Sasaki, S., Iwata, M., 1998. Inducible nitric oxide synthase (iNOS)-like immunoreactivity in argyrophilic, tau-positive astrocytes in progressive supranuclear palsy. Acta Neuropathol. 95, 338–344.

Lin, W.L., Zehr, C., Lewis, J., Hutton, M., Yen, S.-H., Dickson, D.W., 2005. Progressive white matter pathology in the spinal cord of transgenic mice expressing mutant (P301L) human tau. J. Neurocytol. 34, 397–410.

Lue, L.F., Rydel, R., Brigham, E.F., Yang, L.B., Hampel, H., Murphy, G. M.J., Brachova, L., Yan, S.D., Walker, D.G., Shen, Y., Rogers, J., 2001. Inflammatory repertoire of Alzheimer's disease and nondemented elderly microglia in vitro. Glia 35, 72–79.

Morgan, D., Gordon, M.N., Tan, J., Wilcock, D., Rojiani, A.M., 2005. Dynamic complexity of the microglial activation response in transgenic models of amyloid deposition: implications for Alzheimer therapeutics. J. Neuropathol. Exp. Neurol. 64, 743–753.

Moriguchi, S., Mizoguchi, Y., Tomimatsu, Y., Hayashi, Y., Kadowaki, T., Kagamiishi, Y., Katsube, N., Yamamoto, K., Inoue, K., Watanabe, S., Nabekura, J., Nakanishi, H., 2003. Potentiation of NMDA receptor-mediated synaptic responses my microglia. Brain Res. Mol. Brain Res. 119, 160–169.

Murakami, T., Paitel, E., Kawarabayashi, T., Ikeda, M., Chishti, M. A., Janus, C., Matsubara, E., Sasaki, A., Kawarai, T., Phinney, A. L., Harigaya, Y., Horne, P., Egashira, N., Mishima, K., Hanna, A., Yang, J., Iwasaki, K., Takahashi, M., Fujiwara, M., Ishiguro, K., Bergeron, C., Carlson, G.A., Abe, K., Westaway, D., George-Hyslop, P., Shoji, M., 2006. Cortical neuronal and glial pathology in $TgTau^{P301L}$ transgenic mice: neuronal degeneration, memory disturbance, and phenotypic variation. Am. J. Pathol. 169, 1365–1375.

Odawara, T., Iseki, E., Kosaka, K., Akiyama, H., Ikeda, K., Yamamoto, T., 1995. Investigation of tau-2 microglia-like cells in the subcortical nuclei of human neurodegenerative disorders. Neurosci. Lett. 192, 145–148.

Paulus, W., Bancher, C., Jellinger, K., 1993. Microglia reaction in Pick's disease. Neurosci. Lett. 161, 89–92.

Perry, V.H., 1998. A revised view of the central nervous system microenvironment and major histocompatibility complex class II antigen presentation. J. Neuroimmunol. 90, 113–121.

Sasaki, A., Levison, S.W., Ting, J.P.-Y., 1989. Comparison and quantitation of Ia antigen expression on cultured macroglia and ameboid microglia from Lewis rat cerebral cortex: analyses and implications. J. Neuroimmunol. 25, 63–74.

Sasaki, A., Yamaguchi, H., Ogawa, A., Sugihara, S., Nakazato, Y., 1997. Microglial activation in early stages of amyloid b protein deposition. Acta Neuropathol. 94, 316–322.

Sasaki, A., Shoji, M., Harigaya, Y., Kawarabayashi, T., Ikeda, M., Naito, M., Matsubara, E., Abe, K., Nakazato, Y., 2002. Amyloid cored plaques in Tg2576 transgenic mice are characterized by giant plaques, slightly activated microglia and the lack of PHF-typed, dystrophic neuritis. Virchows Archiv 441, 358–367.

Schofield, E., Kersaitis, C., Shephered, C.E., Kril, J.J., Halliday, M., 2003. Severity of gliosis in Pick's disease and frontotemporal

lobar degeneration: tau-positive glia differentiate these disorders. Brain 126, 827–840.

Schwab, C., Hosokawa, M., McGeer, P.L., 2004. Transgenic mice overexpressing amyloid beta protein are an incomplete model of Alzheimer diseases. Exp. Neurol. 188, 52–64.

Takeuchi, H., Wang, J., Kawanokuchi, J., Mitsuma, N., Mizuno, T., Suzumura, A., 2006. Interferon-gamma induces microglia-activation-induced cell death: a hypothetical mechanism of relapse and remission in multiple sclerosis. Neurobiol. Dis. 22, 33–39.

Terry, R.D., 2000. Cell death or synaptic loss in Alzheimer disease. J. Neuropathol. Exp. Neurol. 59, 1118–1119.

Trapp, B.D., Wujek, J.R., Criste, G.A., Jalabi, W., Yin, X., Kidd, G.J., Stohlman, S., Ransohoff, R., 2007. Evidence for synaptic stripping by cortical microglia. Glia 55, 360–368.

Uchihara, T., Tsuchiya, K., Nakamura, A., Arai, T., Ikeda, K., 2000. Appearance of tau-2 immunoreactivity in glial cells in human brain with cerebral infarction. Neurosci. Lett. 286, 99–102.

Uchihara, T., Duyckaerts, C., Seilhean, D., Nakamura, A., Lazarini, F., Hauw, J.-J., 2005. Exclusive induction of tau2 epitope in microglia/macrophages in inflammatory lesions—tautwopathy distinct from degenerative tauopathies. Acta Neuropathol. 109, 159–164.

Yoshiyama, Y., Higuchi, M., Zhang, B., Huang, S.M., Iwata, N., Saido, T.C., Maeda, J., Suhara, T., Trojanowski, J.Q., Lee, V.M., 2007. Synapse loss and microglial activation precede tangles in a P301S tauopathy mouse model. Neuron 53, 337–351.

Zhang, W., Wang, T., Pei, Z., Miller, D.S., Wu, X., Block, M.L., Wilson, B., Zhang, W., Zhou, Y., Hong, J.S., Zhang, J., 2005. Aggregated alpha-synuclein activates microglia: a process leading to disease progression in Parkinson's disease. FASEB J. 19, 533–542.

Zhao, Z., Ho, L., Suh, J., Qin, W., Pyo, H., Pompl, P., Ksiezak-Reding, H., Pasinetti, G.M., 2003. A role of P301L tau mutant in anti-apoptotic gene expression, cell cycle and apoptosis. Mol. Cell. Neurosci. 24, 367–379.

BRAIN RESEARCH 1250 (2009) 232-241

available at www.sciencedirect.com

ScienceDirect

www.elsevier.com/locate/brainres

BRAIN RESEARCH

Research Report

# Motor impairment and aberrant production of neurochemicals in human α-synuclein A30P+A53T transgenic mice with α-synuclein pathology☆

Masaki Ikeda[a], Takeshi Kawarabayashi[b], Yasuo Harigaya[d], Atsushi Sasaki[c], Shuichi Yamada[g], Etsuro Matsubara[e], Tetsuro Murakami[f], Yuya Tanaka[f], Tomoko Kurata[f], Xu Wuhua[f], Kenji Ueda[h], Hisashi Kuribara[i], Yasushi Ikarashi[j], Yoichi Nakazato[c], Koichi Okamoto[a], Koji Abe[f], Mikio Shoji[b,*]

[a]Department of Neurology, Gunma University Graduate School of Medicine, Maebashi, Japan
[b]Department of Neurology, Hirosaki University School of Medicine, Hirosaki, Japan
[c]Department of Human Pathology, Gunma University Graduate School of Medicine, Maebashi, Japan
[d]Department of Neurology, Maebashi Red Cross Hospital, Maebashi, Gunma, Japan
[e]Department of Alzheimer's Disease Research, National Institute for Longevity Sciences, Obu, Japan
[f]Department of Neurology, Neuroscience, Biophysiological Science, Okayama University Graduate School of Medicine and Dentistry, Okayama, Japan
[g]Immuno-Biological Laboratories Co., Ltd., Mikasa, Hokkaidio, Japan
[h]Department of Neural Plasticity, Tokyo Institute of Psychiatry, Setagaya-ku, Tokyo, Japan
[i]Tokyo University of Social Welfare, Isesaki, Japan
[j]R and D Division, Tsumura and Co., Ltd, Inashiki, Japan

ARTICLE INFO

Article history:
Accepted 6 October 2008
Available online 1 November 2008

Keywords:
α-synuclein
Mutation
Transgenic mouse
Parkinson's disease
Neurochemical

ABSTRACT

Missense point mutations, duplication and triplication in the α-synuclein (αSYN) gene have been identified in familial Parkinson's disease (PD). Familial and sporadic PD show common pathological features of αSYN pathologies, e.g., Lewy bodies (LBs) and Lewy neurites (LNs), and a loss of dopaminergic neurons in the substantia nigra that leads to motor disturbances. To elucidate the mechanism of αSYN pathologies, we generated TgαSYN transgenic mice overexpressing human αSYN with double mutations in A30P and A53T. Human αSYN accumulated widely in neurons, processes and aberrant neuronal inclusion bodies. Sarcosyl-insoluble αSYN, as well as phosphorylated, ubiquitinated and nitrated αSYN, was accumulated in the brains. Significantly decreased levels of dopamine (DA) were recognized in the striatum. Motor impairment was revealed in a rotarod test. Thus, TgαSYN is a useful model for analyzing the pathological cascade from aggregated αSYN to motor disturbance, and may be useful for drug trials.



Grant numbers and sources of supports: Supported by **Grant-in-Aid for** Grants-in-Aid for Primary Amyloidosis Research Committee (M. S.), from the Ministry of Health, Labor and Welfare of Japan and by Grants-in-Aid for Scientific Research (B) (M.S.: 19390233, K.A.: 18390257), (C) (M.I.: 19590980, T.K.: 19590976, A.S.: 18500276, E.M.: 18590968), from the Ministry of Education, Culture, Sports, Science and Technology, Japan.

* Corresponding author. Fax: +81 172 39 5143.
E-mail address: mshoji@hirosaki-u.ac.jp (M. Shoji).

0006-8993/$ – see front matter © 2008 Published by Elsevier B.V.
doi:10.1016/j.brainres.2008.10.011

## 1. Introduction

αSYN was originally isolated from senile plaques in Alzheimer's disease as a protein of 35 highly hydrophobic amino acid metabolites, known as the non-amyloid component (NAC), derived from a 140 amino-acid precursor encoded by a gene on chromosome 4 (Ueda et al., 1992; Chen et al., 1995), which has homology to rat and Torpedo αSYN and songbird synelfin (George et al., 1995). αSYN is highly abundant in presynaptic terminals (Iwai et al., 1995) and has potential roles in synaptic function and neural plasticity (George et al., 1995; Clayton and George, 1998).αSYN binds to phospholipid vesicles and inhibits PLD2, a regulator of vesicle membrane budding (Liscovitch et al., 2000; Lotharius and Brundin, 2000; Payton et al., 2000), and also plays modulatory roles in the release of dopamine vesicles (Abeliovich et al., 2000).

A few cases of familial Parkinson's disease (FPD) have been linked to missense point mutations in αSYN with A53T (Polymeropoulos et al., 1997), A30P (Kruger et al., 1998) and E46K (PARK1) (Zarranz et al., 2004). Soon after the first A53T missense mutation of αSYN was discovered, the main component of Lewy bodies (LBs) was identified as insoluble aggregates of αSYN (Baba et al., 1998). αSYN and phosphorylated-Ser129 αSYN accumulated in LBs and Lewy neurites (LNs) in PD and Dementia with Lewy bodies (DLB) (Fujiwara et al., 2002; Hasegawa et al., 2002). Then, a second causative gene known as *parkin* (Kitada et al., 1998) was found in familial autosomal recessive juvenile Parkinson's disease (PARK2). *Parkin* ubiquitinates αSYN normally and this process is aberrantly altered in PD (Shimura et al., 2001). Acceleration of oligomerization or protofibrillization is a common property of mutant αSYN (Conway et al., 2001; Choi et al., 2004). Recently, triplication of the αSYN locus (PARK4) was identified in an "Iowanian kindred" with autosomal dominant Lewy body disease (Singleton et al., 2002). Subsequently, duplication of the αSYN gene locus was also reported as a cause of familial PD (Chartier-Harlin et al., 2004). These findings suggest that overexpression of wild type αSYN also leads to facilitation of insoluble aggregation of αSYN. α-synucleinopathy is a disease entity which shares common pathological accumulation of insoluble aggregates of αSYN in the neurons and processes of PD, DLB, Hallervorden–Spatz disease, pure autonomic failure and in the glial cells of multiple system atrophy (MSA) (Goedert, 2000; Hardy and Gwinn-Hardy, 1998; Spillantini et al., 1997; Tu et al., 1998; Galvin et al., 2000; Shoji et al., 2000; Arai et al., 2000).

To elucidate the pathological mechanism of LBs and LNs associated with the decrease in dopamine (DA) production, it is necessary to investigate the aberrant mechanism of mutant αSYN, which is an essential molecule consisting of LBs and LNs (Baba et al., 1998). Here, we generated transgenic (Tg) mice expressing human mutant αSYN A30P+A53T under a human Thy-1 promoter, named as TgαSYN. Overexpression of double mutant human αSYN was expected to lead to further synergistic effects and induce severe α-synucleinopathies and neurodegeneration (Citron et al., 1998; Chishti et al., 2001). TgαSYN showed significant motor impairment in rotarod test, accumulation of insoluble αSYN, aberrant inclusions and decreased dopamine levels. These findings indicate that TgαSYN is a useful animal model to investigate the crucial pathogenesis of α-synucleinopathies, and it may help to develop therapeutic agents.

## 2. Results

### 2.1. *Expression of αSYN in transgenic mice and analyses of RT-PCR*

We used the transgene construct hThy1-αSYN A30P+A53T to generate transgenic (Tg) mice, TgαSYN (Fig. 1a). PCR analysis of tail-derived DNA revealed 18 positive Tg mice for human αSYN and EGFP among 129 F0 mice. Five of the 18 Tg mice showed the strongest green fluorescence under irradiation at 365 nm ultraviolet (Fig. 1b). These selected independent lines (#8707, #8713, #8718, #8812, #8819) were mated with BDF1 mice and raised for examination. The following Tg mice were analyzed: 18 positive Tg progenies, 60 F1 Tg (#8707: 2, #8713: 31, #8718: 5, #8812: 10, #8819: 12) and 135 F2 Tg (#8707: 0, #8713: 101, #8718: 2, #8812: 29, #8819: 3). The mRNA expressions of human αSYN A30P+A53T and EGFP in TgαSYN brains were confirmed by RT-PCR, showing the same expression levels of human αSYN A30P+A53T and EGFP at three, eight and 17 months old, respectively (Figs. 1c and d). Western blot using LB509 recognized a 16 kD band corresponding to human αSYN only in Tg mice. AB5038 recognized a 16 kD band corresponding to both human and mouse αSYN. The expression level of human αSYN was 130% of that of endogenous mouse αSYN (Fig. 1e).

### 2.2. *Histological studies*

Immunocytochemistry of sagittal sections of a seven-month-old #8707 TgαSYN brain by LB509 revealed extensive human αSYN immunostaining in the brainstem, hippocampus, thalamus, cerebral cortex and cerebellum (Fig. 2a, arrow indicates the substantia nigra), but no staining in the non-Tg mouse (Fig. 2b). The TgαSYN brain showed atrophy of the cerebral cortex and cerebellum (Fig. 2a). The HE stain showed eosinophilic inclusion bodies and vacuoles in the cytoplasm of neurons in the substantia nigra (Fig. 2c, arrow), and in the dentate nucleus of TgαSYN (Fig. 2h, arrow). These cytoplasmic inclusions were stained with human-αSYN specific antibody, LB509 (Fig. 2d, arrow, and Fig. 2i, arrow), and anti-αSYN antibody, 42/α-Synuclein (Fig. 2j, arrows). Nitrated α/β synuclein was also stained in the cytoplasmic inclusions (Fig. 2e, arrow,). Ubiquitin-positive inclusions were observed in neurons at brainstem (Fig. 2f, arrow), and dystrophic neurites in the dentate nucleus of TgαSYN (Fig. 2g). Staining of phosphorylated synuclein showed diffuse staining in somatodendrites of TgαSYN neurons (Fig. 2k). Gallyas–Braak staining revealed dystrophic neurites in the dentate nucleus of TgαSYN (Fig. 2l) in ubiquitin-positive structures in the same region (Fig. 2g). Anti-tyrosine hydroxylase (TH) immuno-positive neurons in the locus ceruleus showed weak immunostaining intensity in TgαSYN (Fig. 2m), compared with those of non-Tg mice brains (Fig. 2n). The intensity of substance P immunopositive synapses in the striata of TgαSYN brains (Fig. 2o) was weaker than that of non-Tg mice brains (Fig. 2p). Severe astrocytosis

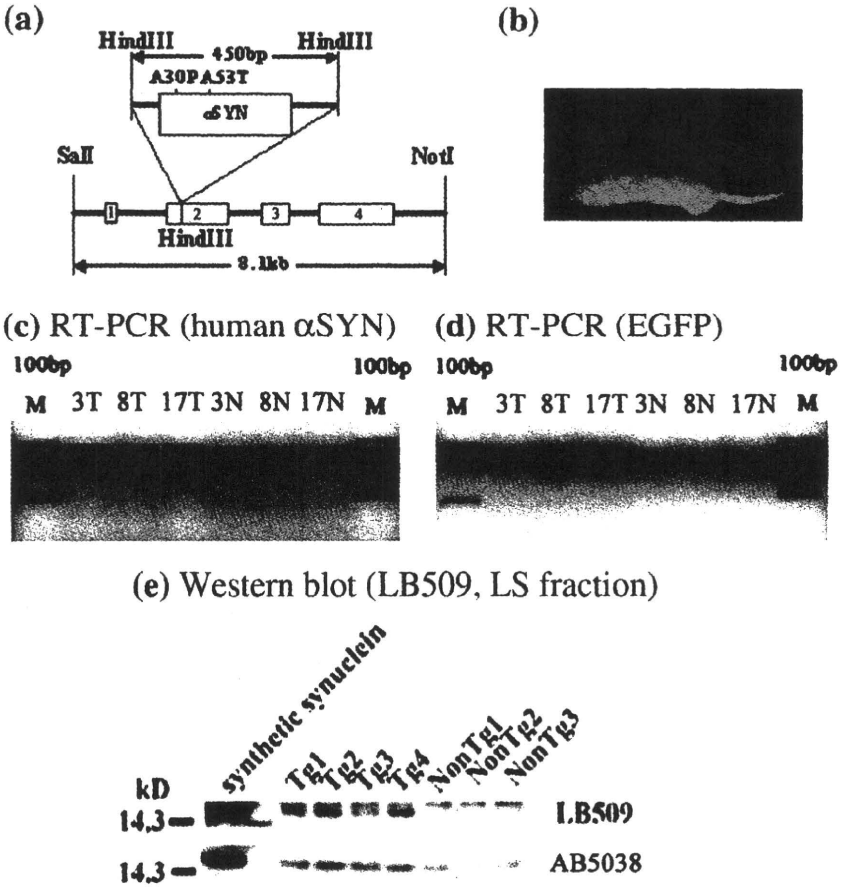


**Fig. 1 – The mutant αSYN A30P+A53T construct and the expression of EGFP. (a) The structure of the construct: hThy1-αSYN A30P+A53T. (b) TgαSYN (#8713) showed fluorescence by EGFP (enhanced green fluorescence protein) under 365 nm long wave UV (EGFP-negative non-Tg mouse in the upper location, EGFP-positive Tg mouse in the lower location). (c) Analyses of RT-PCR transcripts: Human αSYN mRNA transcripts (exons 2–4) were detected as 280 bp in TgαSYN brains, but not in non-Tg mice brains, and the intensity of PCR products was the same level as three-, eight-, and 17-month-old Tg mice brains. (d) EGFP mRNA transcripts were detected in TgαSYN brains at the same level at three, eight and 17 months of age, but not in non-Tg mice brains (N showed non-Tg mice brains, T showed Tg mice brains). (e) The expression of human αSYN was detected as a 16 kD band at the same size as recombinant synthetic αSYN by Western blot using LB509 in LS-soluble fractions of TgαSYN #8713 (Tg1–4) mice brains, but not in three 14-month-old non-Tg mice brains (upper lane). AB5038 recognized a 16 kD band corresponding to human and mouse αSYN (lower lane). The expression level of human αSYN was about 130% of that of endogenous mouse αSYN. Synthetic αSYN (SS) was used as a marker of 16 kD αSYN (BIOMOL Research Laboratories Inc., Plymouth Meeting, PA).**

was observed in the cerebellum of a 16-month-old TgαSYN (Fig. 2q). An EM study demonstrated cytoplasmic inclusions (Fig. 2r, arrow) and intranuclear inclusions (Fig. 2s, arrows) in the neurons of the brainstem. These inclusion bodies lacked the typical halo and fibrillar structure of LBs.

### 2.3. *Western blot analysis*

Fourteen-month-old TgαSYN showed a 16 kD band corresponding to αSYN in the LS-soluble fraction (L), Triton-soluble fraction (T), sarcosyl-soluble (S) and sarcosyl-insoluble fractions (I) (Fig. 3a: arrow). In sarcosyl-insoluble fraction, smear pattern was detected in TgαSYN#8812(T3), which accumulated much synuclein histologically. The anti-phosphorylated αSYN antibody pSyn#64 labeled the same size band as αSYN, 16 kD (Fig. 3b: arrow). These findings presented that sarcosyl-insoluble human αSYN and phosphorylated αSYN was accumulated in TgαSYN brains as reported in DLB brains (Hasegawa et al., 2002).

### 2.4. *Rotarod test for motor function of TgαSYN*

The rotarod test demonstrated that significant motor impairment appeared after a shorter time in TgαSYN; they dropped from the rotating rod faster than non-Tg littermates. The motor impairment was found at three months of age ($p<0.01$) and thereafter deteriorated with age ($p<0.001$. Fig. 4).

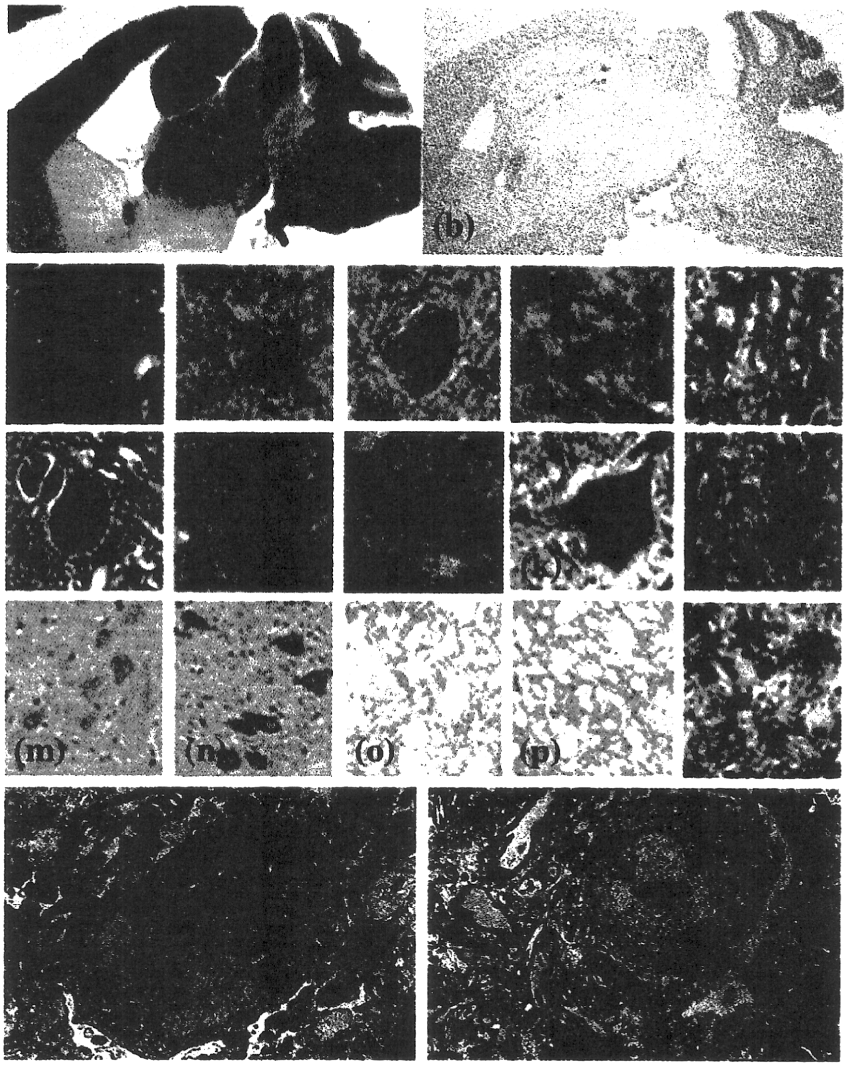


**Fig. 2 – The pathological features of TgαSYN at seven months of age and age-matched non-Tg mice. (a) A sagittal section of a seven-month-old #8707 TgαSYN brain labeled by LB509 showed extensive αSYN accumulation prominently in the brainstem, hippocampus, thalamus, cerebellum and cerebral cortex. The substantia nigra of the midbrain is also labeled (arrow). The cerebral cortex and cerebellum showed atrophy. (b) No staining in the non-Tg mice brain by LB509. (c) Hematoxylin–eosin stain showed eosinophilic inclusion bodies and vacuoles in the cytoplasm of neurons in the substantia nigra of #8707 TgαSYN (arrow). (d) LB509 detected cytoplasmic inclusions in the substantia nigra of #8707 TgαSYN (arrow). (e) Anti-nitrated α/β SYN monoclonal antibody (Syn12) immunostained cytoplasmic inclusions in the substantia nigra (arrow), as well as in 14-month-old #8713 TgαSYN. (f) Ubiquitin-positive inclusions are shown in the substantia nigra of #8707 TgαSYN (arrow). (g) Ubiquitin-positive dystrophic neurites in the cerebellum dentate of 16-month-old #8713 TgαSYN. (h) Eosinophilic cytoplasmic inclusions (arrow) in the dentate nucleus of #8707 TgαSYN. (i) LB509-positive inclusion in the dentate nucleus of #8707 TgαSYN (arrow). (j) Cytoplasmic inclusions immunostained with a mouse monoclonal antibody 42/α-Synuclein in the brainstem of #8812 TgαSYN (arrow). (k) The PSer129 αSYN antibody immunostained the cytoplasm of neurons in the substantia nigra of #8707 TgαSYN. (l) Gallyas–Braak stain of dystrophic neurites in the dentate nucleus of a 16-month-old #8713 TgαSYN. (m) Tyrosine hydroxylase (TH) immuno-positive neurons in the locus ceruleus showed less immunostaining in the #8707 TgαSYN brain, than the non-Tg mouse brain (n). (o) The intensity of substance P immuno-positive synapses in the striatum of #8707 TgαSYN brain was lower than non-Tg mice brain (p). (q) Astrocytosis in the cerebellum of 16-month-old #8713 TgαSYN. (r) Electron-dense inclusions were found in the cytoplasm of neurons in the brainstems of 8-month-old #8718 TgαSYN by an EM study (arrow). (s) In the brainstem of the same mouse, intracellular inclusions (arrows) were also detected. Scale bar = 1 mm in a, b, 12.5 μm in c–f, h–k, 50 μm in g, l, m, n, 25 μm in o, p, and 0.38 μm in r, s.**

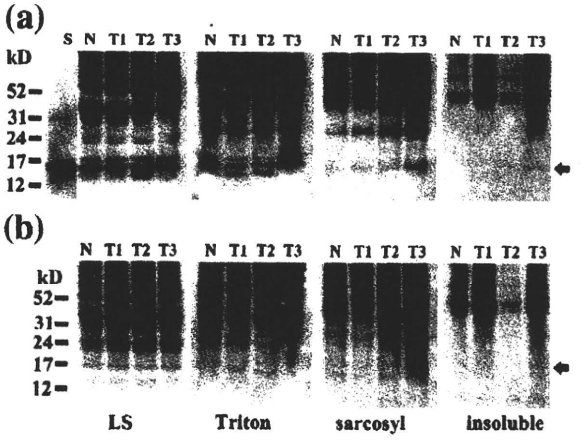


**Fig. 3 – Western blot analysis. The expression of human αSYN was 16 kD (lane S; corresponded to recombinant human αSYN) by Western blot using antibody LB509 (a) and pSyn#64 (b) in LS-soluble (L), Triton-soluble (T), sarcosyl-soluble (S) and sarcosyl-insoluble (I) fractions of non-Tg (N), TgαSYN#8713 (T1), TgαSYN#8819 (T2), and TgαSYN#8812 (T3), 14-month-old mice brains.**

### 2.5. *Measurement of neurochemicals*

There was no significant difference in brain weight among Tg and non-Tg mice at 10 and 17 months of age. Compared with age-matched non-Tg control mice, the levels of DA in the striatum were significantly decreased in 10 month-old ($p=0.0159$) and 17 month-old mice brains ($p=0.0286$). DA decreased approximately 17% to 24% in the striatum of TgαSYN brains (Fig. 5a). A significant decrease in DA was also detected in the hypothalamuses of 17-month-old TgαSYN brains ($p=0.0079$. Fig. 5b). NE was not decreased in any areas of 10-month-old TgαSYN brains (Fig. 5c). Serotonin was decreased in the hypothalamuses of 10- and 17-month-old TgαSYN brains ($p=0.0079$, $p=0.0286$, respectively. Fig. 5d). ACh decreased in the striatum in 17-month-old TgαSYN ($p=0.0286$. Fig. 5e). There was no significant alteration in DOPAC, HVA, MHPG, 5-HIAA and Ch levels in any areas of TgαSYN (data not shown). These results showed that insoluble mutant αSYN aggregation selectively decreased the DA level at 10 and 17 months of age.

## 3. Discussion

Several groups have already reported animal models of PD, such as wild-type αSYN Tg mice (Masliah et al., 2000), mutant αSYN Tg mice (van der Putten et al., 2000, Kahle et al., 2000, Giasson et al., 2002, Lee et al., 2002, Richfield et al., 2002, Neumann et al., 2002, Thiruchelvam et al., 2004, Tofaris et al. 2006, Wakamatsu et al., 2008), *Drosophila melanogaster* (Pendleton et al., 2002) and *C. elegans* (Kuwahara et al., 2006). The first αSYN Tg mice expressed wild-type human αSYN driven by the PDGF-β promoter (Masliah et al., 2000). This mouse displayed intraneuronal inclusions immunoreactive for αSYN and ubiquitin in several regions typically affected in α-synucleinopathies, while lacking the characteristic fibrillar components of Lewy bodies. The Tg mice overexpressing αSYN A53T developed under the murine Thy-1 regulatory sequence showed an early and dramatic decline in motor function (van der Putten et al., 2000). Transgenic wild-type and A30P αSYN abnormally accumulated in neuronal cell bodies and neurites throughout the brain (Kahle et al., 2000). Mice expressing wild-type or A53T αSYN under the mouse prion promoter developed motor deficits by eight months of age (Giasson et al., 2002). Neuropathological assessment of these Tg mice revealed a wide distribution of αSYN, with a pathological sparing of the motor cortex and a total sparing of the substantia nigra. Another group developed Tg mice harboring αSYN A53T using a mouse prion promoter showing motor dysfunction and αSYN accumulation (Lee et al., 2002). Truncated human αSYN (C-120) Tg mice under the TH promoter led to pathological changes in dopaminergic nerve cells of the substantia nigra and olfactory bulb (Tofaris et al., 2006). Recently, truncated human αSYN (C-130) Tg mice also led to selective loss of dopaminergic neurons and accumulation of phosphorylated αSYN (Wakamatsu et al., 2007, 2008).

One of the differences between these models and our TgαSYN was a novel combination of a promoter and mutation of αSYN. TgαSYN expressed double mutant αSYN with A30P +A53T under the human Thy-1 promoter. As expected, our TgαSYN demonstrated widespread αSYN accumulation in the brainstem, caudate putamen, cerebellum, hippocampus and cerebral cortex. Eosinophilic inclusion bodies in the substantia nigra and dentate nucleus of the cerebellum corresponded to accumulation of αSYN. Accumulated αSYN was ubiquitinated, nitrated and phosphorylated at the histological levels as shown in PD and DLB brain. Unfortunately, these inclusion bodies were not compatible with typical LBs because of the absence of a halo structure. At the EM level, fibrillar structure was not observed in inclusion bodies, but they were composed of massive aberrant fine granular structures. Aberrant inclusion bodies with modified αSYN were also observed widely. Since Gallyas–Braak staining labeled these LNs, accumulated αSYN in these neurites may have characteristics of those in β-sheet pleated structures.

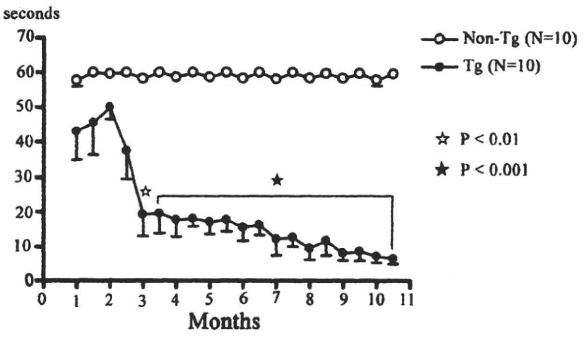


**Fig. 4 – Rotarod test. The retention time of Tg mice on the rotarod significantly decreased in TgαSYN. The significant difference began to decrease at three months old (☆: $p<0.01$) and progressively deteriorated in an age-dependent manner from six months (★: $p<0.001$). Statistics were analyzed by two-way repeated measures ANOVA.**

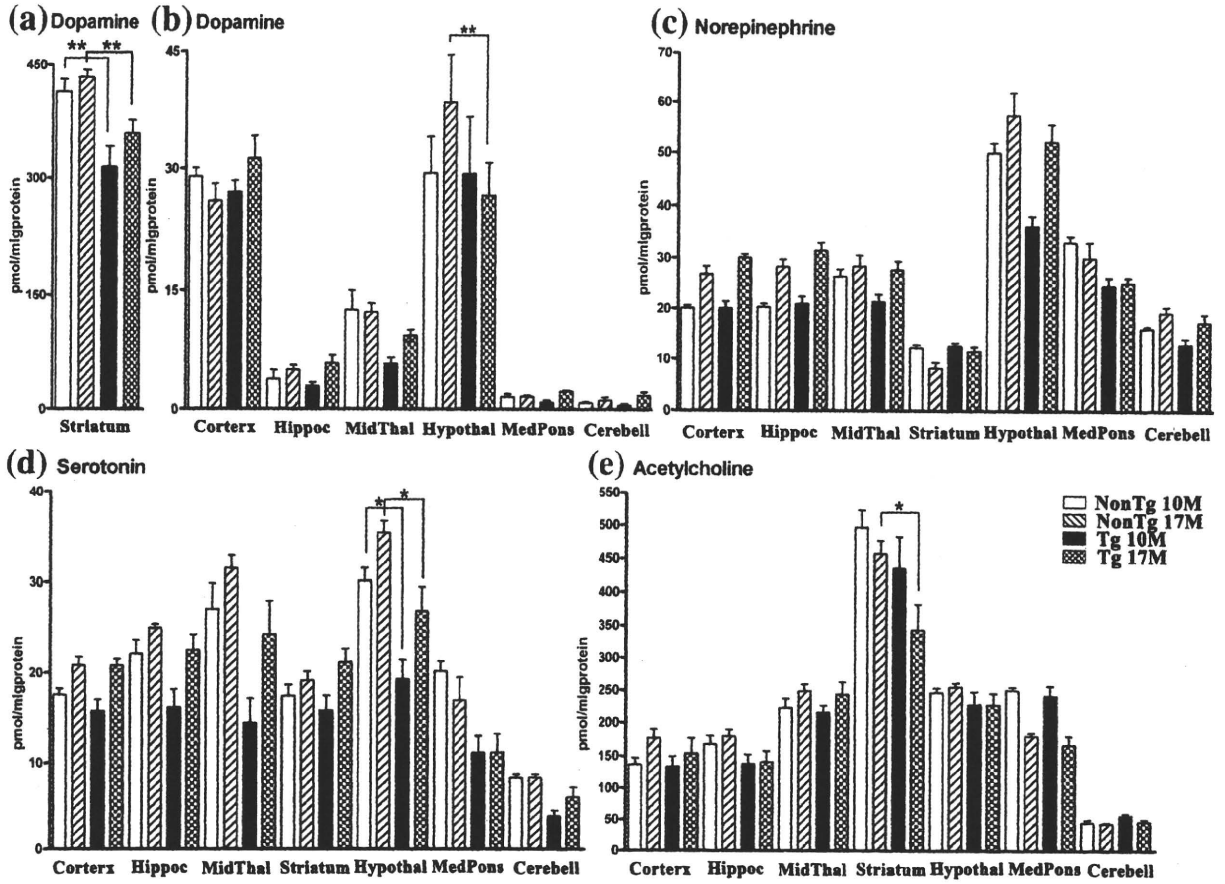


**Fig. 5 – Measurement of neurochemicals. Opened column: 10-month-old non-Tg mice, Oblique column: 17-month-old non-Tg mice; Closed black colored column: 10-month-old TgαSYN mice, Crossed column: 17-month-old non-Tg mice. Cortex: cerebral cortex, Hippoc: hippocampus, MidThal: midbrain–thalamus, Hypothal: hypothalamus, MedPons: medulla–pons, Cerebell: cerebellum. *$p<0.01$, **$p<0.05$. Statistical analysis of neurochemicals between the TgαSYN and non-Tg control groups at the same age was conducted by a two-way repeated measure ANOVA (GraphPad Prism 4). (a) DA was significantly decreased in the striatum in 10- and 17-month-old TgαSYN compared with non-Tg control mice. (b) A decrease in dopamine was detected significantly in the hypothalamuses of 17-month-old TgαSYN brains ($p=0.0079$). (c) Norepinephrine (NE) was not decreased in 10- and 17-month-old TgαSYN brains. (d) Serotonin (5-HT) was decreased in the hypothalamus of 10- and 17-month-old TgαSYN brains ($p=0.0079$, $p=0.0286$, respectively). (e) ACh was decreased in the striatum of 17-month-old TgαSYN ($p=0.0286$).**

The α-synuclein pathologies in TgαSYN were accompanied by decreased tyrosine hydroxylase-positive neurons, Substance P synapses and severe astrocytosis. These histological α-synuclein pathologies were also detected at the biochemical level. Accumulated αSYN was phosphorylated, ubiquitinated and sarcosyl-insoluble, suggesting that it may be conformationally changed as reported in PD/DLB brains (Hasegawa et al., 2002). The presence of higher molecule phosphorylated and ubiquitinated bands (22/29 kD) on Western blots also indicated that accumulated αSYN was modified and aggregated.

The severe decrease in DA and loss of dopaminergic neurons in SNc and the striata of PD brains is widely believed to be the pathological and biochemical cause of PD. Notably, our TgαSYN demonstrated decreased DA production in a disturbed DA system which was measured in the liquid chromatographic systems. Although other neurochemicals were altered slightly, a prominently decreased level of DA was revealed in the striatum of TgαSYN. These findings suggest selective neurotoxicity with αSYN accumulation.

In our mouse model, approximately a 20% reduction in DA in the striatum was observed when motor impairment existed. Since the rotarod test revealed significant decreased spontaneous movement, the phenotype of TgαSYN is quite similar to the cardinal clinical symptom of PD, akinesia. A decreased level of TH-positive neurons and substance P synapses also suggested that the motor impairment in TgαSYN may be caused by aberrant αSYN processes.

Our TgαSYN is a mammalian model animal showing decreased DA and motor deficits, which were certainly detected by the liquid chromatographic systems and rotarod test. For this reason, TgαSYN is a useful model for analyzing the aberrant cascade induced by pathological metabolism and aggregation of mutant αSYN, and may be useful for developing essential treatments for α-synucleinopathies such as PD and DLB.

## 4. Experimental procedures

### 4.1. *Transgene construction, generation of transgenic mice and analyses of RT-PCR*

Human αSYN A30P+A53T cDNA (450 bp) was ligated into Hind III sites in the human Thy-1 genome gene. The transgene hThy1-αSYN A30P+A53T consisted of an 8.1 kb XhoI–NcoI fragment of pBluescript II KS kidney enhancer (Fig. 1a). The CX-EGFP transgene consisted of a 3 kb Xba I/BamH I fragment of pCAGGS containing the CMV enhancer, β-actin promoter, a part of the rabbit β-globin gene, a part of the second intron, the third exon and 3′-untranslated region and cDNA of EGFP (Enhanced green fluorescent protein) with the Kozak sequence (Imai et al., 1999). Approximately 2,000 copies of the transgene with a 1:1 mole rate mixture of the hThy1-αSYN A30P+A53T and CX-EGFP as a transgene marker were micro-injected into the pronuclei of fertilized BDF1 eggs. To analyze gene expression of human αSYN, RT-PCR was performed using 2 μl of mRNA, isolated using the QuickPrep Micro mRNA purification kit (GE Healthcare Bio-Sciences Corp., Piscataway, NJ), from the brains of TgαSYN (#8713) and non-Tg mice brains at 3, 8, 17 months of age ($n=3$, respectively) in the reaction tube of Ready-To-Go RT-PCR Beads (GE Healthcare Bio-Sciences Corp., Piscataway, NJ) with PCR primer sets as follows: (αSYN forward primer: TG GAT GTA TTC ATG AAA GGA, αSYN reverse primer: CC AGT GGC TGC TGC AAT GCT C; EGFP forward primer: TGG TGA GCA AGG GCG AGG AG; EGFP reverse primer: TCG TGC TGC TTC ATG TGG TC). For semi-quantification, RT-PCR of β-actin was performed as an internal control (Elliott, 2001). Ten microliters of PCR products were analyzed by 2.5% agarose gel electrophoresis. The intensity of ethidium-stained bands was analyzed by Scion Image (Scion Corporation, Frederick, MD).

### 4.2. *Histological examinations*

After mice were sacrificed under anesthesia, the brains were removed and cut sagittally along the midline. One hemisphere was fixed in 0.1 mol/L phosphate buffer (PB, pH 7.6) containing 4% paraformaldehyde, and embedded in paraffin. For immunostaining, 5-μm sections were treated with 99% formic acid for 3 min, or treated in a microwave at 500 W for 5 min three times in 10 mmol/L citrate buffer (pH 6.0). After blocking with 5% normal goat or horse serum in 50 mmol/L phosphate buffered saline (PBS) containing 0.05% Tween-20 and 4% Block-Ace (Snow brand, Sapporo, Japan), sections were incubated with primary antibodies for 6 h. Specific labeling was visualized using a Vectastain Elite ABC kit (Vector, Burlingame, CA). Immunostained tissue sections were counterstained with hematoxylin. Nissl, Hematoxylin–eosin (H–E), and Gallyas–Braak stains were also done.

The following antibodies were used: mouse monoclonal antibody to human αSYN, LB509 (×4, residues 115–121/122) (Baba et al., 1998); mouse monoclonal antibody to αSYN, 42/α-Synuclein (×50, BD Transduction Laboratories, San Jose, CA); rabbit polyclonal antibody to phosphorylated Serine at residue 129 of human αSYN, PSer129 (×200) (Fujiwara et al., 2002; Hasegawa et al., 2002); rabbit polyclonal antibody to tyrosine hydroxylase (TH), AB151 (×2,000, CHEMICON, Temecula, CA); rabbit polyclonal antibody to substance P, AB1566 (×1,000, CHEMICON, Temecula, CA); rabbit polyclonal antibody to ubiquitin, UbiQ (×500) (Ikeda et al., 2005; Murakami et al., 2006); mouse monoclonal antibody to nitrated α/β SYN, Syn12 (×400, Invitrogen, Corps., Carlsbad, CA); rabbit polyclonal antibody to glial fibrillary acidic protein (GFAP, ×20,000, DAKO, Carpinteria, CA).

For electron microscopic (EM) studies, the brain tissues were immersed in a fixative solution (2.5% glutaraldehyde, 0.1 mol/L phosphate buffer (PB), pH 7.4) for 4 h and washed several times in 0.1 mol/L PB containing 7% sucrose. Blocks were then postfixed in 2% osmium tetroxide, dehydrated in ethanol and propylene oxide, and embedded in Quetol 812 (Nisshin EM, Tokyo, Japan). Ultrathin sections were stained with uranyl acetate and lead acetate prior to observation.

### 4.3. *Western blot analysis*

Half of each brain was homogenized in 3 ml/g of low-salt buffer (LS: 10 mmol/L Tris, 5 mmol/L ethylenediaminetetraacetic acid (EDTA), 1 mmol/L dithiothreitol (DTT), 10% sucrose, and a cocktail of protease inhibitors (Complete®, Roche Diagnostics, Indianapolis, IN), pH 7.5) and centrifuged at 25,000 g for 30 min at 4 °C (LS-soluble fraction). Pellets were treated with 3 ml/g of LS with 1% Triton X-100 and 0.5 mol/L NaCl, and centrifuged at 180,000 g for 30 min at 4 °C (Triton-soluble fraction). Pellets were then homogenized again in 2 ml/g LS with 1% N-lauroylsarcosine (SIGMA CHEMICAL CO. St Louis, MO) and 0.5 mol/L NaCl, incubated at 22 °C on a shaker for 1 h, and centrifuged at 180,000 g for 30 min at 22 °C. Supernatants were analyzed as sarcosyl-soluble fraction (Iwatsubo et al., 1996; Hasegawa et al., 2002; Sampathu et al., 2003; Ikeda et al., 2005; Murakami et al., 2006). The remaining pellets obtained from each sarcosyl-insoluble fraction were boiled at 70 °C in 20 μl of NuPAGE® LDS Sample Buffer for 10 min. Each fraction was separated on 4 to 12% NuPAGE Bis–Tris Gels (Invitrogen, Corps., Carlsbad, CA) and the blots were labeled by a mouse monoclonal antibody to human αSYN (LB509, ×4), and a mouse monoclonal antibody to phosphorylated Serine at residue 129 of human αSYN (pSyn#64, ×200, Wako, Japan). Signals were visualized with an enhanced chemiluminescence detection system (SuperSignal West® Dura Extended Duration Substrate, PIERCE, Rockford, IL) and quantified by a luminoimage analyzer (LAS 1000-mini, Fuji film, Tokyo, Japan).

### 4.4. *Measurement of neurochemicals*

Neurochemicals, including dopaminergic (dopamine: DA, 3,4-dihydroxyphenylacetic acid: DOPAC, homovanillic acid: HVA), noradrenergic (norepinephrine: NE, 3-methoxy-4hydroxyphenylglycol: MHPG), serotonergic (5-hydroxytryptamine: 5-HT, 5-hydroxyindoleacetic acid: 5-HIAA) and cholinergic (acetylcholine: ACh, choline: Ch) systems in the brain were measured in Tg mice ($n=10$) and non-Tg control mice ($n=10$) at 10 and 17 months old, respectively. In brief, each animal was anesthetized with Nembutal® (Dainippon Pharmaceutical Co. Ltd., pentobarbital sodium), sacrificed, and irradiated with microwaves (NJE 2603 Microwave device, New Japan Radio, Kamifukuoka, Japan) at 9.0 kW for 0.42 s to prevent post-mortem